THE
SOCIETY

MEMOIRS

OF THE

COLLEGE OF SCIENCE

KYOTO IMPERIAL UNIVERSITY

SERIES A

VOL. XIV, NO. 5

SEPTEMBER 1931

KYOTO

On a Unified Theory of Gravitational and Electromagnetic Fields

By

Shūjiro Kunii

(Received July 6, 1931)

Abstract

The object of this paper is to unify the gravitational and electromagnetic fields in a simple way and to deduce equations of motion of charged particles as well as those of light-rays.

To do this, the writer makes the following assumptions:

(i) Our space-time world is a four-dimensional continuum with a semi-symmetric and metric connection, whose fundamental tensor $g_{\mu\nu}$ and vector φ_ν are interpreted as the gravitational and electromagnetic potentials respectively.

(ii) The field-laws are derived from a Hamiltonian function $R-L$, where R is the scalar curvature of the world and L is an invariant formed by $g_{\mu\nu}$ and φ_ν.

Starting from these assumptions and applying several mathematical theorems, the writer shows that all the results given in the theory of general relativity together with Maxwell-Lorentz's theory are obtained in a compact form without any modification.

An attractive theory based on parallelism at a distance has been published by Einstein[1] a few years ago. To develope his theory he used the conception of an orthogonal ennuple, which was also used by Levi-Civita,[2] and he succeeded in finding the field-equations in the first approximation, but he could not find the equations of the path traced by a particle carrying an electric charge. Other theories starting from the notion of infinitesimal parallel displacement have been developed by Weyl,[3] Eddington[4] and also by Einstein.[5]

But by these theories it is not possible to compare lengths (except

1. A. Einstein: Berlin. Berichte, 1 (1929)
2. T. Levi-Civita: Berlin. Berichte, 138 (1929)
3. H. Weyl: Berlin. Berichte, 465 (1918)
4. A. S. Eddington: Proc. Roy. Soc. A. **99**, 104 (1921)
5. A. Einstein: Berl. Berichte, 32, 76, 137 (1923)

zero length) at different points, because the length of any vector is changed by a parallel displacement. Though Einstein's new theory is free from this difficulty, it seems unnatural and complicated in its geometrical structure.

In this paper we try to show that Einstein's celebrated equations of the gravitational field and Maxwell-Lorentz's equations of the electromagnetic field in the relativistic form can be admitted without modification in a four dimensional continuum having the characteristic properties such that the fundamental tensor- and vector fields may exist and the comparison of lengths at different points is possible, and also to show that the equations of the path traced by a particle carrying a charge can be deduced, in an ordinary form, by means of energy-momentum-equations. Our unification of the gravitational and electromagnetic fields is accomplished by using a differential geometry which is a special case of a very general one based on the principle of linear connection given by Schouten.[1]

In 1928 Leopordo Infeld[2] had already attacked the problem by the aid of a differential geometry which is contained in Schouten's as another special case and obtained the field-equations in a slightly different form. But the writer thinks that the following theory is more simple and complete than the line of approach adopted by Infeld.

§ 1. Geometrical preliminaries.

In this section we describe briefly our geometrical theory in the manner in which it is extended by Schouten.[3] Suppose an n-dimensional continuum defined by any ordered set of n independent real variables $x^{\nu}(\nu=1, 2, \ldots\ldots, n)$, which are called the coordinates of points in it. Moreover, consider that this continuum obeys the principle of linear connection; a connection which satisfies the following five conditions is called a linear one:—

(i) Any tensor and its absolute differential are tensors of the same kind.

We denote the absolute differential of any tensor Φ by the symbol $\delta\Phi$, and its ordinary differential by the symbol $d\Phi$.

---

1. J. A. Schouten: Der Ricci-Kalcül.
2. L. Infeld: Zs. f. Phys., **50**, 137 (1928)
3. loc. cit. Chap. II.
   Schouten established his theory discriminating the "eigentlich" tensor from the ordinary one. But in our case we need not consider this difference, so as to develope the concept of the "Überschiebungsinvariant" connection.

(ii) The absolute differential of any tensor is a linear function of coordinate differentials.

(iii) The absolute differential of a sum is the sum of the absolute differentials of its components, thus

$$\delta(\Phi+\Psi)=\delta\Phi+\delta\Psi.$$

(iv) The absolute differentiation of an outer product obeys the same rule as the ordinary differentiation, namely

$$\delta(\Phi\Psi)=\Psi\delta\Phi+\Phi\delta\Psi.$$

(v) The absolute differential of any invariant is equal to its ordinary differential: viz.

$$\delta A=dA,$$

where A is an invariant.

When the absolute differential of any tensor Φ is expressed by the form

$$\delta\Phi=dx^{\mu}\nabla_{\mu}\Phi,$$

we may call $\nabla_{\mu}\Phi$ the covariant derivative of Φ. In the foregoing connection Schouten showed that the absolute differentials of any contravariant vector A^{ν} and any covariant vector B_{ν} are respectively given by the formulae[1]

$$\delta A^{\nu}=dA^{\nu}+\Gamma^{\nu}_{\lambda\mu}A^{\lambda}dx^{\mu}$$
$$\delta B_{\nu}=dB_{\nu}-\Gamma'^{\lambda}_{\nu\mu}B_{\lambda}dx^{\mu},$$

where $\Gamma^{\nu}_{\lambda\mu}$ and $\Gamma'^{\nu}_{\lambda\mu}$ are $2n^3$ arbitrarily chosen functions of x's.

Let us confine ourselves to the consideration of the case which Schouten called the "Überschiebungsinvariant" connection i. e. $\Gamma^{\nu}_{\lambda\mu}=\Gamma'^{\nu}_{\lambda\mu}$, and call it simply "the connection". Then, in our connection, we have

$$\delta A^{\nu}=dA^{\nu}+\Gamma^{\nu}_{\lambda\mu}A^{\lambda}dx^{\mu}, \qquad (1\cdot1)$$

and

$$\delta B_{\nu}=dB_{\nu}-\Gamma^{\lambda}_{\nu\mu}B_{\lambda}dx^{\mu}, \qquad (1\cdot2)$$

from which it can easily be shown that, if $A^{\beta_1\cdots\cdots\beta_q}_{\alpha_1\cdots\cdots\alpha_p}$ are the components of a tensor, its absolute differential is given by

$$\delta A^{\beta_1\cdots\cdots\beta_q}_{\alpha_1\cdots\cdots\alpha_p}=dA^{\beta_1\cdots\cdots\beta_q}_{\alpha_1\cdots\cdots\alpha_p}+\sum_{i=1}^{q}\Gamma^{\beta_i}_{\lambda\mu}A^{\beta_1\cdots\beta_{i-1}\lambda\beta_{i+1}\cdots\beta_q}_{\alpha_1\cdots\cdots\alpha_p}dx^{\mu}$$
$$-\sum_{j=1}^{p}\Gamma^{\lambda}_{\alpha_j\mu}A^{\beta_1\cdots\cdots\beta_q}_{\alpha_1\cdots\alpha_{j-1}\lambda\alpha_{j+1}\cdots\alpha_p}dx^{\mu}. \qquad (1\cdot3)$$

1. loc. cit. p. 65.

If we express the preceding formulae (1·1), (1·2) and (1·3) in forms of covariant derivatives, we have

$$\nabla_\mu A^\nu = \frac{\partial A^\nu}{\partial x^\mu} + \Gamma^\nu_{\lambda\mu} A^\lambda, \tag{1·4}$$

$$\nabla_\mu B_\nu = \frac{\partial B_\nu}{\partial x^\mu} - \Gamma^\lambda_{\nu\mu} B_\lambda, \tag{1·5}$$

and

$$\nabla_\mu A^{\beta_1 \cdots \beta_q}_{\alpha_1 \cdots \alpha_p} = \frac{\partial A^{\beta_1 \cdots \beta_q}_{\alpha_1 \cdots \alpha_p}}{\partial x^\mu} + \sum_{i=1}^{q} \Gamma^{\beta_i}_{\lambda\mu} A^{\beta_1 \cdots \beta_{i-1} \lambda \beta_{i+1} \cdots \beta_q}_{\alpha_1 \cdots \alpha_p} - \sum_{j=1}^{p} \Gamma^{\lambda}_{\alpha_j \mu} A^{\beta_1 \cdots \beta_q}_{\alpha_1 \cdots \alpha_{j-1} \lambda \alpha_{j+1} \cdots \alpha_p} \tag{1·6}$$

Applying (1·6) to the tensor δ^ν_λ (=1 for $\lambda=\nu$; =0 for $\lambda \neq \nu$), we get

$$\nabla_\mu \delta^\nu_\lambda = \Gamma^\nu_{\lambda\mu} - \Gamma^\nu_{\lambda\mu} = 0, \tag{1·7}$$

which is the characteristic property of our connection.

Our connection is then determinate, when the coefficients of connection $\Gamma^\nu_{\lambda\mu}$ are defined as functions of the coordinates x's. In order that the connection may itself be independent of the choice of coordinates, the set of n^3 functions $\Gamma^\nu_{\lambda\mu}$ must be transformed, in a definite way, into another set of n^3 functions $\bar{\Gamma}^\nu_{\lambda\mu}$ if we take another system of coordinates x's.

It is evident that the transformation-equations of the Γ's are given by

$$\bar{\Gamma}^\nu_{\lambda\mu} = \Gamma^\alpha_{\beta\tau} \frac{\partial x^\beta}{\partial \bar{x}^\lambda} \frac{\partial x^\tau}{\partial \bar{x}^\mu} \frac{\partial \bar{x}^\nu}{\partial x^\alpha} + \frac{\partial^2 x^\alpha}{\partial \bar{x}^\lambda \partial \bar{x}^\mu} \frac{\partial \bar{x}^\nu}{\partial x^\alpha}, \tag{1·8}$$

when we perform a transformation of coordinates

$$\bar{x}^\alpha = \bar{x}^\alpha(x^1, x^2, \ldots\ldots, x^n)$$

whose Jacobian is not identically zero.

According to (1·8) it follows that the difference

$$2P^\nu_{\lambda\mu} \equiv \Gamma^\nu_{\lambda\mu} - \Gamma^\nu_{\mu\lambda} \tag{1·9}$$

is also a tensor of the third rank which is anti-symmetric with respect to λ and μ. In particular, we say that the connection is semi-symmetric, when $P^\nu_{\lambda\mu}$ has the following form

$$P^\nu_{\lambda\mu} = \frac{1}{2}(\varphi_\lambda \delta^\nu_\mu - \varphi_\mu \delta^\nu_\lambda), \tag{1·10}$$

where φ_λ are the components of a vector.

As in Riemannian geometry, if we define the curl of a vector A_ν by the tensor of the second rank $\nabla_\mu A_\nu - \nabla_\nu A_\mu$, we obtain, in a semi-symmetric connection,

$$\nabla_\mu A_\nu - \nabla_\nu A_\mu = \left(\frac{\partial A_\nu}{\partial x^\mu} - \frac{\partial A_\mu}{\partial x^\nu}\right) - \varphi_\nu A_\mu + \varphi_\mu A_\nu. \tag{1·11}$$

From this it follows that the curl of the fundamental vector φ_ν is

$$\nabla_\mu \varphi_\nu - \nabla_\nu \varphi_\mu = \frac{\partial \varphi_\nu}{\partial x^\mu} - \frac{\partial \varphi_\mu}{\partial x^\nu}. \tag{1·12}$$

It is a remarkable fact that in our semi-symmetric connection only the curl of the fundamental vector φ_ν has the same form as in Riemannian geometry, as we have just seen.

In the preceding arguments we have obtained the tensor-field $P_{\lambda\mu}^{\nu}$ formed by the fundamental vector-field φ_ν as in (1·10), but it is not sufficient to determine the $\Gamma_{\lambda\mu}^{\nu}$-field by means of a single vector-field φ_ν. After Schouten, this determination of the $\Gamma_{\lambda\mu}^{\nu}$-field can be accomplished by the aid of the vector-field φ_ν and a certain tensor-field.

If we take any symmetric contravariant tensor $g^{\lambda\nu}$ whose determinant g has rank n, there exists a unique covariant tensor $g_{\lambda\nu}$ which is defined as the cofactor of $g^{\lambda\nu}$ in this determinant, divided by g. Hence we have

$$g_{\lambda\mu} g^{\mu\nu} = \delta_\lambda^\nu. \tag{1·13}$$

For the covariant derivatives of $g^{\lambda\nu}$ and $g_{\lambda\nu}$, we use the symbols $Q_\mu^{\lambda\nu}$ and $S_{\mu\lambda\nu}$ respectively: viz

$$\left.\begin{aligned} \nabla_\mu g^{\lambda\nu} &= Q_\mu^{\lambda\nu}, \\ \nabla_\mu g_{\lambda\nu} &= S_{\mu\lambda\nu}. \end{aligned}\right\} \tag{1·14}$$

Differentiating (1·13) covariantly and substituting (1·14) in it, we get

$$S_{\mu\lambda\nu} = -g_{\lambda\alpha} g_{\nu\beta} Q_\mu^{\alpha\beta}.$$

Accordingly the two sets of equations

$$Q_\mu^{\lambda\nu} = \frac{\partial g^{\lambda\nu}}{\partial x^\mu} + \Gamma_{\alpha\mu}^{\lambda} g^{\alpha\nu} + \Gamma_{\alpha\mu}^{\nu} g^{\lambda\alpha} = 0 \tag{1·15}$$

and

$$S_{\mu\lambda\nu}=\frac{\partial g_{\lambda\nu}}{\partial x^{\mu}}-\Gamma^{\alpha}_{\lambda\mu}g_{\alpha\nu}-\Gamma^{\alpha}_{\nu\mu}g_{\lambda\alpha}=0 \qquad (1\cdot16)$$

are equivalent to one another.

If $\Gamma^{\nu}_{\lambda\mu}$ satisfy (1·16) or (1·15), we call this connection a metric one. Although we can determine $\Gamma^{\nu}_{\lambda\mu}$, as Schouten showed[1], by the two general tensor-fields $P_{\lambda\mu}^{\ \ \nu}$ and $Q_{\mu}^{\lambda\nu}$, we may express $\Gamma^{\nu}_{\lambda\mu}$ with these only when the connection is semi-symmetric and metric.

In this case $\Gamma^{\nu}_{\lambda\mu}$ satisfies (1·16) i. e.

$$\Gamma^{\alpha}_{\mu\nu}g_{\lambda\alpha}+\Gamma^{\alpha}_{\lambda\nu}g_{\mu\alpha}=\frac{\partial g_{\lambda\mu}}{\partial x^{\nu}}. \qquad (1\cdot17)\text{a}$$

Similarly

$$\Gamma^{\alpha}_{\nu\lambda}g_{\mu\alpha}+\Gamma^{\alpha}_{\mu\lambda}g_{\nu\alpha}=\frac{\partial g_{\mu\nu}}{\partial x^{\lambda}}, \qquad (1\cdot17)\text{b}$$

$$\Gamma^{\alpha}_{\lambda\mu}g_{\nu\alpha}+\Gamma^{\alpha}_{\nu\mu}g_{\lambda\alpha}=\frac{\partial g_{\lambda\nu}}{\partial x^{\mu}}. \qquad (1\cdot17)\text{c}$$

Adding (1·17)b and (1·17)c and subtracting (1·17)a, we obtain by (1.9)

$$2\Gamma^{\alpha}_{\lambda\mu}g_{\nu\alpha}=\left(\frac{\partial g_{\lambda\nu}}{\partial x^{\mu}}+\frac{\partial g_{\mu\nu}}{\partial x^{\lambda}}-\frac{\partial g_{\lambda\mu}}{\partial x^{\nu}}\right)+2(P_{\lambda\mu}^{\ \ \alpha}g_{\nu\alpha}+P_{\mu\nu}^{\ \ \alpha}g_{\lambda\alpha}+P_{\lambda\nu}^{\ \ \alpha}g_{\mu\alpha}),$$

where $P_{\lambda\mu}^{\ \ \nu}$ is, of course, given by (1·10).

If we solve $\Gamma^{\nu}_{\lambda\mu}$ from the above equations and use (1·10), we can easily show that

$$\Gamma^{\nu}_{\lambda\mu}=\left\{\begin{matrix}\nu\\ \lambda\mu\end{matrix}\right\}+\varphi_{\lambda}\delta^{\nu}_{\mu}-g_{\lambda\mu}\varphi^{\nu}, \qquad (1\cdot18)$$

where $\left\{\begin{matrix}\nu\\ \lambda\mu\end{matrix}\right\}$ is the Christoffel 3-index-symbol formed with $g_{\mu\nu}$, and φ^{ν} is the associated vector of φ_{λ} with respect to $g_{\mu\nu}$. (Hereafter we will use these notations as in Riemannian geometry.)

From (1·18) it will be seen that the coefficients of connection are completely determined by the vector-field φ_{ν} and the tensor-field $g_{\mu\nu}$.

If we put

$$\varphi_{\lambda}\delta^{\nu}_{\mu}-g_{\lambda\mu}\varphi^{\nu}=T_{\lambda\mu}^{\ \ \nu}, \qquad (1\cdot19)$$

we have, from (1·18),

$$\Gamma^{\nu}_{\lambda\mu}=\left\{\begin{matrix}\nu\\ \lambda\mu\end{matrix}\right\}+T_{\lambda\mu}^{\ \ \nu}. \qquad (1\cdot20)$$

---

1. loc. cit. pp. 72–73

According to the tensorial property of $T_{\lambda\mu}^{\nu}$ defined by (1·19), we infer that the quantities $\mathring{\nabla}_{\mu}A^{\nu}$ and $\mathring{\nabla}_{\mu}B_{\nu}$ defined by

$$\left.\begin{aligned}\mathring{\nabla}_{\mu}A^{\nu}&=\frac{\partial A^{\nu}}{\partial x^{\mu}}+\left\{\begin{matrix}\nu\\ \alpha\mu\end{matrix}\right\}A^{\alpha},\\ \mathring{\nabla}_{\mu}B_{\nu}&=\frac{\partial B_{\nu}}{\partial x^{\mu}}-\left\{\begin{matrix}\alpha\\ \nu\mu\end{matrix}\right\}B_{\alpha}\end{aligned}\right\} \tag{1·21}$$

are also tensors of the second rank, since the covariant derivatives of these vectors A^{ν} and B_{ν} can be written in the form

$$\left.\begin{aligned}\nabla_{\mu}A^{\nu}&=\mathring{\nabla}_{\mu}A^{\nu}+T_{\alpha\mu}^{\nu}A^{\alpha},\\ \nabla_{\mu}B_{\nu}&=\mathring{\nabla}_{\mu}B_{\nu}-T_{\nu\mu}^{\alpha}B_{\alpha}.\end{aligned}\right\} \tag{1·22}$$

In particular, if we contract (1·22) with respect to μ and ν, we have

$$\nabla_{\nu}A^{\nu}=\mathring{\nabla}_{\nu}A^{\nu}+(n-1)\varphi_{\nu}A^{\nu}. \tag{1·23}$$

Evidently these formulae can be extended, without difficulty, to the covariant derivatives of a tensor of any rank.

§ 2. Theory of continuum with a semi-symmetric and metric connection.

In our n-dimensional continuum let C be any curve defined by the equations

$$x^{\nu}=x^{\nu}(t),$$

where t is a parameter. As in Riemannian Geometry, a unique solution A^{ν} of the system of differential equations

$$\frac{dA^{\nu}}{dt}+\Gamma_{\lambda\mu}^{\nu}A^{\lambda}\frac{dx^{\mu}}{dt}=0, \tag{2·1}$$

satisfying the initial conditions

$$A^{\nu}(t_0)=\overset{0}{A}{}^{\nu},$$

where $\overset{0}{A}{}^{\nu}$ is any given vector at a point t_0 of C is said to be a family of vectors parallel along C to the given vector $\overset{0}{A}{}^{\nu}$ at the point t_0 of C.

By (1·1) the system of differential equations (2·1) is obviously equivalent to the system

$$\delta A^{\nu}=0. \tag{2·2}$$

Hence the absolute change of the squared length A^2 of the vector A^{ν} defined by

$$A^2=g_{\mu\nu}A^{\mu}A^{\nu} \tag{2·3}$$

is $\delta g_{\mu\nu}A^\mu A^\nu$, when A^μ is carried by an infinitesimal parallel displacement. But this value is evidently zero, since our connection satisfies the metric conditions (1·16) i. e. $\delta g_{\mu\nu}=0$.

Similarly, if we define the angle θ between any two vectors A^μ and B^ν by the equation

$$\cos\theta=g_{\mu\nu}A^\mu B^\nu \qquad (2\cdot 4)$$

we can prove that its absolute change is also zero. Therefore we get the theorem: The length of a vector and the angle between two vectors do not change their values respectively through the parallel displacement of the vectors along any given curve. This makes it possible to compare lengths and angles at different points without any ambiguity.

Accordingly, if we define the length of C by the integral $\int_c ds$, it has a definite meaning and when we choose it as a parameter of C, $\frac{dx^\nu}{ds}$ gives the tangent-vector of C whose length is always unity.

If we introduce the contravariant vector

$$N^\nu=\frac{d^2x^\nu}{ds^2}+\Gamma^\nu_{\lambda\mu}\frac{dx^\lambda}{ds}\frac{dx^\mu}{ds}, \qquad (2\cdot 5)$$

it is obvious that $N^\nu ds$ represents the absolute differential of the tangent vector of C. Accordingly we call N^ν the principal normal of C.

When $N^\nu=0$ along C, the curve is said to be a geodesic. Strictly speaking, geodesics are curves such that the absolute changes of their tangent-vectors along them are identically zero.

Hence we have

$$\frac{d^2x^\nu}{ds^2}+\Gamma^\nu_{\lambda\mu}\frac{dx^\lambda}{ds}\frac{dx^\mu}{ds}=0, \qquad (2\cdot 6)$$

as the differential equations of geodesics.

But by means of the relation

$$\varphi_\lambda\frac{dx^\lambda}{ds}\frac{dx^\nu}{ds}=\varphi^\nu$$

and (1·18), equations (2·5) and (2·6) can be written as

$$N^\nu=\frac{d^2x^\nu}{ds^2}+\left\{\begin{matrix}\nu\\ \lambda\mu\end{matrix}\right\}\frac{dx^\lambda}{ds}\frac{dx^\mu}{ds} \qquad (2\cdot 7)$$

and

$$\frac{d^2x^\nu}{ds^2}+\left\{\begin{matrix}\nu\\ \lambda\mu\end{matrix}\right\}\frac{dx^\lambda}{ds}\frac{dx^\mu}{ds}=0 \qquad (2\cdot 8)$$

respectively.

In particular, when a curve of zero-length satisfies the differential equations of the form (2·8), in which s is simply used as a parameter of the curve, we will call it a minimal geodesic.

From what has been said, it will be seen that the expressions of the principal normal of a curve and the differential equations of a geodesic in our geometry are of the same form as in Riemannian Geometry.

We are now going to construct the curvature tensor in our connection.

In order to do this, take a surface defined by

$$x^\nu=f^\nu(u, v)$$

where the functions f^ν and their derivatives up to the third order exist and are continuous at a point P, and consider a circuit passing through this point $P(u, v)$, $Q(u+\Delta u, v)$, $R(u+\Delta u, v+\Delta v)$, $S(u, v+\Delta v)$ and P. If a vector A^ν is transported parallel to itself around this circuit, it is well known that the difference $\Delta(A^\nu)_P$ of the final and initial values at P of the components of the vector A^ν is given by the equations

$$\Delta(A^\nu)_P=\left(A^\lambda R^\nu{}_{\lambda\mu\sigma}\frac{\partial x^\sigma}{\partial u}\frac{\partial x^\mu}{\partial v}\right)_P\Delta u\Delta v, \qquad (2\cdot 9)$$

where $R^\nu{}_{\lambda\mu\sigma}$ is called the curvature tensor of the continuum and is given by

$$R^\nu{}_{\lambda\mu\sigma}=\frac{\partial\Gamma^\nu_{\lambda\sigma}}{\partial x^\mu}-\frac{\partial\Gamma^\nu_{\lambda\mu}}{\partial x^\sigma}+\Gamma^\varkappa_{\lambda\sigma}\Gamma^\nu_{\varkappa\mu}-\Gamma^\varkappa_{\lambda\mu}\Gamma^\nu_{\varkappa\sigma}. \qquad (2\cdot 10)$$

Since our continuum is subjected to a semi-symmetric and metric connection, we must substitute (1·18) for the $\Gamma^\nu_{\lambda\mu}$ in the right hand side of (2·10). And, after a tedious calculation, we can show that

$$\begin{aligned}R^\nu{}_{\lambda\mu\sigma}=B^\nu{}_{\lambda\mu\sigma}&+\delta^\nu_\sigma\nabla_\mu\varphi_\lambda-\delta^\nu_\mu\nabla_\sigma\varphi_\lambda-g_{\lambda\sigma}\nabla_\mu\varphi^\nu\\&+g_{\lambda\mu}\nabla_\sigma\varphi^\nu+(\delta^\nu_\mu g_{\lambda\sigma}-\delta^\nu_\sigma g_{\lambda\mu})\Phi,\end{aligned} \qquad (2\cdot 11)$$

where $B^\nu{}_{\lambda\mu\sigma}$ is the Riemann-Christoffel tensor formed by $g_{\lambda\mu}$, i. e.

$$B^\nu{}_{\lambda\mu\sigma}=\frac{\partial}{\partial x^\mu}\left\{\begin{matrix}\nu\\ \lambda\sigma\end{matrix}\right\}-\frac{\partial}{\partial x^\sigma}\left\{\begin{matrix}\nu\\ \lambda\mu\end{matrix}\right\}+\left\{\begin{matrix}\varkappa\\ \lambda\sigma\end{matrix}\right\}\left\{\begin{matrix}\nu\\ \varkappa\mu\end{matrix}\right\}-\left\{\begin{matrix}\varkappa\\ \lambda\mu\end{matrix}\right\}\left\{\begin{matrix}\nu\\ \varkappa\sigma\end{matrix}\right\} \qquad (2\cdot 12)$$

and Φ is the squared length of φ_ν, i.e.

$$\Phi=\varphi_\nu\varphi^\nu. \tag{2·13}$$

Writing

$$R^\sigma{}_{\lambda\mu\sigma}=R_{\lambda\mu} \tag{2·14}$$

and

$$B^\sigma{}_{\lambda\mu\sigma}=G_{\lambda\mu}, \tag{2·15}$$

we get the contracted tensor

$$R_{\lambda\mu}=G_{\lambda\mu}+(n-2)\nabla_\mu\varphi_\lambda+g_{\lambda\mu}\nabla_\nu\varphi^\nu-(n-1)g_{\lambda\mu}\Phi, \tag{2·16}$$

whose symmetrical part $K_{\lambda\mu}$ and anti-symmetrical part $F_{\lambda\mu}$ are respectively given by

$$K_{\lambda\mu}=G_{\lambda\mu}+\frac{n-2}{2}(\nabla_\mu\varphi_\lambda+\nabla_\lambda\varphi_\mu)+g_{\lambda\mu}\nabla_\nu\varphi^\nu-(n-1)g_{\lambda\mu}\Phi \tag{2·17}$$

and

$$F_{\lambda\mu}=\frac{n-2}{2}(\nabla_\mu\varphi_\lambda-\nabla_\lambda\varphi_\mu). \tag{2·18}$$

Multiplying (2·16) by $g^{\lambda\mu}$, we get

$$R=G+2(n-1)\nabla_\nu\varphi^\nu-n(n-1)\Phi, \tag{2·19}$$

where we put

$$R=g^{\lambda\mu}R_{\lambda\mu}, \tag{2·20}$$

and

$$G=g^{\lambda\mu}G_{\lambda\mu}. \tag{2·21}$$

In particular, for $n=4$, we can reduce these formulae to a more simple form, viz.

$$R_{\lambda\mu}=G_{\lambda\mu}+2\nabla_\mu\varphi_\lambda+g_{\lambda\mu}\nabla_\nu\varphi^\nu-3g_{\lambda\mu}\Phi, \tag{2·22}$$

$$K_{\lambda\mu}=G_{\lambda\mu}+(\nabla_\mu\varphi_\lambda+\nabla_\lambda\varphi_\mu)+g_{\lambda\mu}\nabla_\nu\varphi^\nu-3g_{\lambda\mu}\Phi, \tag{2·23}$$

$$F_{\lambda\mu}=\nabla_\mu\varphi_\lambda-\nabla_\lambda\varphi_\mu, \tag{2·24}$$

$$R=G+6\nabla_\nu\varphi^\nu-12\Phi. \tag{2·25}$$

From (2·24) it will be seen that the anti-symmetrical part $F_{\lambda\mu}$ of the contracted curvature tensor $R_{\lambda\mu}$ is the curl of the fundamental vector φ_ν. Accordingly, in consequence of (1·12), we can write it

$$F_{\lambda\mu}=\frac{\partial\varphi_\lambda}{\partial x^\mu}-\frac{\partial\varphi_\mu}{\partial x^\lambda}. \tag{2·26}$$

§ 3. Field-equations.

The construction of our physical theory depends on the following assumptions.

(i) Our space-time world is a four-dimensional continuum with a semi-symmetric and metric connection.

(ii) We interpret the fundamental tensor $g_{\lambda\mu}$ and vector φ_ν as the gravitational potentials and the electromagnetic potential-vector respectively.

(iii) The field-laws in our space-time world are describable by two systems of such differential equations that the Lagrangian derivatives of a scalar-density $\mathfrak{H}$, called the Hamiltonian function, with respect to $g^{\lambda\mu}$ and φ_ν are proportional to the energy-tensor-density $\mathfrak{T}_{\lambda\mu}$ and charge-current vector-density $\mathfrak{S}^\nu$ respectively.

First let us adopt as the Hamiltonian function $\mathfrak{H}$

$$\mathfrak{H}\equiv H\sqrt{-g}=(R-L)\sqrt{-g}, \tag{3·1}$$

where R is the scalar curvature of our space-time world given by (2·25) and

$$L=\frac{\varkappa}{2}F_{\alpha\beta}F^{\alpha\beta}+6\Phi, \tag{3·2}$$

$F_{\alpha\beta}$ and Φ being given by (2·24) and (2·13) respectively and $\varkappa$ a universal constant.

Then let us consider the variation of the Hamiltonian integral

$$I=\int \mathfrak{H}\, dx, \tag{3·3}$$

where $dx\equiv dx^1dx^2dx^3dx^4$, in a region for arbitrary small variations $\delta g^{\lambda\mu}$ and $\delta\varphi_\nu$ under the conditions that they will vanish with their first derivatives at the boundary of the region.

In consequence of (2·25), (3·1) and (3·3), the variation of I is given by

$$\begin{aligned}\delta I&=\delta\int(R-L)\sqrt{-g}\,dx\\&=\delta\int\left(G+6\nabla_\nu\varphi^\nu-18\Phi-\frac{\varkappa}{2}F_{\alpha\beta}F^{\alpha\beta}\right)\sqrt{-g}\,dx.\end{aligned} \tag{3·4}$$

Applying (1·23) to the fundamental vector φ^ν, we have

$$\nabla_\nu\varphi^\nu=\mathring{\nabla}_\nu\varphi^\nu+3\Phi.$$

Hence we get

$$(\Gamma_\nu\varphi^\nu)\sqrt{-g}=\frac{\partial}{\partial x^\nu}(\sqrt{-g}\varphi^\nu)+3\Phi\sqrt{-g}.$$

Substituting this in (3·4), we obtain

$$\delta I=\delta\int\left(G-\frac{\chi}{2}F_{\alpha\beta}F^{\alpha\beta}\right)\sqrt{-g}\,dx+6\delta\int\frac{\partial}{\partial x^\nu}(\sqrt{-g}\varphi^\nu)dx.$$

But by the boundary conditions, the second term in the right hand side of the above equation vanishes.

Hence we get

$$\delta I=\delta\int\left(G-\frac{\chi}{2}F_{\alpha\beta}F^{\alpha\beta}\right)\sqrt{-g}\,dx. \qquad (3\cdot5)$$

If we denote the Lagrangian derivatives of $\mathfrak{H}$ with respect to $g^{\lambda\mu}$ and φ_ν by the symbols $[\mathfrak{H}]_{\lambda\mu}$ and $[\mathfrak{H}]^\nu$ respectively, δI can be written

$$\delta I=\int\{[\mathfrak{H}]_{\lambda\mu}\delta g^{\lambda\mu}+[\mathfrak{H}]^\nu\delta\varphi_\nu\}\,dx.$$

From this it follows that the Lagrangian derivatives of $\mathfrak{H}$ with respect to $g^{\lambda\mu}$ and φ_ν are equal to those of $\left(G-\frac{\chi}{2}F_{\alpha\beta}F^{\alpha\beta}\right)\sqrt{-g}$ respectively.

Since

$$\frac{1}{\sqrt{-g}}\left[\left(G-\frac{\chi}{2}F_{\alpha\beta}F^{\alpha\beta}\right)\sqrt{-g}\right]_{\lambda\mu}=G_{\lambda\mu}-\frac{1}{2}g_{\lambda\mu}G$$
$$-\chi\left(g^{\alpha\beta}F_{\lambda\alpha}F_{\mu\beta}-\frac{1}{4}g_{\lambda\mu}F_{\alpha\beta}F^{\alpha\beta}\right)$$

and

$$\frac{1}{\sqrt{-g}}\left[\left(G-\frac{\chi}{2}F_{\alpha\beta}F^{\alpha\beta}\right)\sqrt{-g}\right]^\nu=2\chi\mathring{\nabla}_\sigma F^{\nu\sigma}$$

are well known formulae[1] in the theory of general relativity, we have

$$\frac{1}{\sqrt{-g}}[\mathfrak{H}]_{\lambda\mu}=G_{\lambda\mu}-\frac{1}{2}g_{\lambda\mu}G-\chi\left(g^{\alpha\beta}F_{\lambda\alpha}F_{\mu\beta}-\frac{1}{4}g_{\lambda\mu}F_{\alpha\beta}F^{\alpha\beta}\right) \qquad (3\cdot6)$$

and

$$\frac{1}{\sqrt{-g}}[\mathfrak{H}]^\nu=2\chi\mathring{\nabla}_\sigma F^{\nu\sigma}, \qquad (3\cdot7)$$

where $\mathfrak{H}\equiv\left(R-\frac{\chi}{2}F_{\alpha\beta}F^{\alpha\beta}-6\Phi\right)\sqrt{-g}.$

1. A. S. Eddington: The mathematical theory of Relativity, 2nd. ed., §60, §79.

Now, according to our assumption (iii), we propose

$$\left.\begin{aligned} \frac{1}{\sqrt{-g}}[\mathfrak{H}]_{\lambda\mu} &= -\varkappa T_{\lambda\mu} \\ \frac{1}{\sqrt{-g}}[\mathfrak{H}]^{\nu} &= 2\varkappa S^{\nu} \end{aligned}\right\} \qquad (3\cdot 8)$$

as the field-equations.

By (3·6) and (3·7), the above equations (3·8) can be put in the following form

$$G_{\lambda\mu} - \frac{1}{2} g_{\lambda\mu} G = -\varkappa\left(T_{\lambda\mu} - g^{\alpha\beta} F_{\lambda\alpha} F_{\mu\beta} + \frac{1}{4} g_{\lambda\mu} F_{\alpha\beta} F^{\alpha\beta} \right), \qquad (3\cdot 9)$$

$$\mathring{\nabla}_{\sigma} F^{\nu\sigma} = S^{\nu}, \qquad (3\cdot 10)$$

which are identical with those given by the general theory of relativity. In order to express (3·10) with our covariant derivatives instead of those of Riemannian Geometry, we use the identities

$$\nabla_{\sigma} F^{\nu\sigma} = \mathring{\nabla}_{\sigma} F^{\nu\sigma} + 2\varphi_{\sigma} F^{\nu\sigma},$$

which can easily be shown by (1·6) and (1·18).

Hence the Maxwell-Lorentz equation (3·10) can also be written

$$\nabla_{\sigma} F^{\nu\sigma} - 2\varphi_{\sigma} F^{\nu\sigma} = S^{\nu}. \qquad (3\cdot 11)$$

§ 4. Laws of conservation.

By the so-called "Kastenexperiment" Einstein proposed the equivalence hypothesis, which says that with an appropriately chosen local reference frame special relativity holds for every infinitesimal four-dimensional domain of the world. Evidently this assumption of Einstein's corresponds to the mathematical theorem: In a Riemannian continuum, a system of coordinates can be chosen for which the Christoffel 3-index-symbols i. e. the coefficients of the Riemannian connection, vanish at any given point.

Taking a step further, it is an interesting problem for us to ask whether a reference frame on which the gravitational and electromagnetic phenomena have no influence can exist or not. This is the same as asking whether a system of coordinates for which the coefficients of our semi-symmetric and metric connection vanish at any given point can exist or not.

If such a system of coordinates could be chosen in our connection, the transformed $\overline{\Gamma}^{\nu}_{\lambda\mu}$ would be symmetric with respect to λ and

μ, as can easily be seen by (1·8). Hence at the point considered, $\bar{P}_{\lambda\mu}^{\nu}=0$. From the tensorial property of $P_{\lambda\mu}^{\nu}$, it follows that $P_{\lambda\mu}^{\nu}$ would be zero for any coordinates i. e. our connection would be a symmetric one. This contradicts our assumption. Hence it is not possible to choose a system of coordinates for which the coefficients of our connection vanish at any given point. Of course, the non-existence of such a coordinate system will be also assured by the aid of a general theorem[1]: When, and only when, at a point the coefficients of a connection are symmetric in the subscripts, coordinate systems can be chosen, with the point as origin, such that the coefficients are zero at the point.

From this very important fact we infer that, when the law of conservation is satisfied by a tensor $M_{\lambda\mu}$, its mathematical form is not

$$\nabla_{\nu}M_{\lambda}^{\nu}=0,$$

but

$$\mathring{\nabla}_{\nu}M_{\lambda}^{\nu}=0.$$

For, if we select a sufficiently small region of our space-time world, the law of conservation must be written at least in the form of vanishing of elementary divergence

$$\frac{\partial M_{\lambda}^{1}}{\partial x^{1}}+\frac{\partial M_{\lambda}^{2}}{\partial x^{2}}+\frac{\partial M_{\lambda}^{3}}{\partial x^{3}}+\frac{\partial M_{\lambda}^{4}}{\partial x^{4}}=0.$$

If we interpret

$$M_{\lambda\mu}=T_{\lambda\mu}-g^{\alpha\beta}F_{\lambda\alpha}F_{\mu\beta}+\frac{1}{4}g_{\lambda\mu}F_{\alpha\beta}F^{\alpha\beta} \qquad (4\cdot1)$$

as the whole energy-momentum-tensor, it will consist of two parts $T_{\lambda\mu}$ due to matter and $E_{\lambda\mu}$ due to electromagnetic field, where

$$E_{\lambda\mu}=-g^{\alpha\beta}F_{\lambda\alpha}F_{\mu\beta}+\frac{1}{4}g_{\lambda\mu}F_{\alpha\beta}F^{\alpha\beta}. \qquad (4\cdot2)$$

Since, by means of (4·1), (3·9) can be written in the form

$$G_{\lambda\mu}-\frac{1}{2}g_{\lambda\mu}G=-\varkappa M_{\lambda\mu},$$

and the Riemannian divergence of $\left(G_{\lambda\mu}-\frac{1}{2}g_{\lambda\mu}G\right)$ is identically zero, we obtain

1. L. P. Eisenhart: Non-Riemannian geometry (1927), §20.

$$\left.\begin{aligned} &\mathring{V}_\nu \mathfrak{M}_\lambda^{\ \nu}=0, \\ \text{or}\quad &\frac{\partial \mathfrak{M}_\lambda^{\ \nu}}{\partial x^\nu}+\frac{1}{2}\mathfrak{M}_{\alpha\beta}\frac{\partial g^{\alpha\beta}}{\partial x^\lambda}=0, \end{aligned}\right\} \qquad (4\cdot 3)$$

as representing the law of conservation of the whole energy-momentum-tensor.

Similarly from the identity

$$\mathring{V}_\nu \mathring{V}_\sigma F^{\nu\sigma}=0,$$

it follows that the charge-current-vector S^ν satisfies the law of conservation

$$\left.\begin{aligned} &\mathring{V}_\nu S^\nu=0, \\ \text{or}\quad &\frac{\partial \mathfrak{S}^\nu}{\partial x^\nu}=0. \end{aligned}\right\} \qquad (4\cdot 4)$$

According to the theory of integral invariants, if I is an (absolute) integral invariant such that

$$I=\int W\sqrt{-g}\,dx,$$

where W is an invariant function involving only $g^{\lambda\mu}$ and φ_ν and their derivatives as its arguments, its Lagrangian derivatives with respect to $g^{\lambda\mu}$ and φ_ν satisfy identically the Lie differential equations[1]

$$[\mathfrak{W}]_{\alpha\beta}\frac{\partial g^{\alpha\beta}}{\partial x^\lambda}+[\mathfrak{W}]^\alpha\frac{\partial \varphi_\alpha}{\partial x^\lambda}+\frac{\partial}{\partial x^\alpha}\left\{2[\mathfrak{W}]_{\lambda\beta}g^{\alpha\beta}-[\mathfrak{W}]^\alpha\varphi_\lambda\right\}=0. \qquad (4\cdot 5)$$

If we adopt H given by $(3\cdot 1)$ as W in $(4\cdot 5)$, we get, by $(3\cdot 8)$,

$$\frac{\partial \mathfrak{T}_\lambda^{\ \alpha}}{\partial x^\alpha}+\frac{1}{2}\frac{\partial g^{\alpha\beta}}{\partial x^\lambda}\mathfrak{T}_{\alpha\beta}+\mathfrak{S}^\alpha\left(\frac{\partial \varphi_\lambda}{\partial x^\alpha}-\frac{\partial \varphi_\alpha}{\partial x^\lambda}\right)+\varphi_\lambda\frac{\partial \mathfrak{S}^\alpha}{\partial x^\alpha}=0.$$

Applying $(2\cdot 26)$ and $(4\cdot 4)$ to this, we get

$$\frac{\partial \mathfrak{T}_\lambda^{\ \alpha}}{\partial x^\alpha}+\frac{1}{2}\mathfrak{T}_{\alpha\beta}\frac{\partial g^{\alpha\beta}}{\partial x^\lambda}+F_{\lambda\alpha}\mathfrak{S}^\alpha=0, \qquad (4\cdot 6)$$

and, subtracting this from $(4\cdot 3)$, we obtain

$$\frac{\partial \mathfrak{E}_\lambda^{\ \alpha}}{\partial x^\alpha}+\frac{1}{2}\mathfrak{E}_{\alpha\beta}\frac{\partial g^{\alpha\beta}}{\partial x^\lambda}-F_{\lambda\alpha}\mathfrak{S}^\alpha=0. \qquad (4\cdot 7)$$

These are exactly the same equations as we have already obtained and are known as representing the fact that the rate of change of

1. R. Weitzenböck: Invariantentheorie (1923), Chap. XIV, § 5.

momentum of matter per unit volume is equal to the total ponderable force exerted upon it by the field (for $\mu=1, 2, 3$) and the rate of change of energy of matter per unit volume is equal to the rate at which work is done by this force. (for $\mu=4$)

§ 5. Equations of motion.

In order to find the equations of the path traced by a particle carrying an electric charge, it is enough to pursue the same course as that of general relativity.

Let us consider the case of incoherent matter

$$\mathfrak{T}_\lambda^{\ \alpha}=\mu_0 u_\lambda u^\alpha \sqrt{-g}, \tag{5·1}$$

where μ_0 is the proper density of mass and u^ν is the tangent-vector of the track

$$u^\nu=\frac{dx^\nu}{ds}, \tag{5·2}$$

and assume

$$\mathfrak{S}^\nu=\rho_0 u^\nu \sqrt{-g} \tag{5·3}$$

for the vector-density of charge and current, where ρ_0 is the proper-density of electric charge.

As is well known, if we substitute (5·1), (5·2) and (5·3) in (4·6), we get

$$\mu_0\sqrt{-g}\frac{du_\lambda}{ds}+u_\lambda\frac{\partial}{\partial x^\nu}(\mu_0\sqrt{-g}u^\nu)$$
$$=\frac{1}{2}\frac{\partial g_{\alpha\beta}}{\partial x^\lambda}\mu_0\sqrt{-g}\,u^\alpha u^\beta-F_{\lambda\alpha}\rho_0\sqrt{-g}\,u^\alpha, \tag{5·4}$$

and, multiplying u^λ to (5·4), the law of conservation of proper-mass

$$\frac{\partial}{\partial x^\nu}(\mu_0\sqrt{-g}\,u^\nu)=0 \tag{5·5}$$

can be obtained.

From (5·4) and (5·5), we finally get

$$\frac{d^2x^\nu}{ds^2}+\left\{\begin{matrix}\nu\\ \alpha\beta\end{matrix}\right\}\frac{dx^\alpha}{ds}\frac{dx^\beta}{ds}=-\frac{1}{\mu_0}F^\nu_{\ \alpha}S^\alpha, \tag{5·6}$$

as the differential equations of a world-line taken by a particle carrying a charge. These equations (5·6) are formally identical with those of general relativity.

By (2·5) and (2·7), (5·6) can be written in the form

$$N^{\nu} = -\frac{1}{\mu_0} F^{\nu}{}_{\alpha} S^{\alpha}, \tag{5·7}$$

which shows that the principal normal of a world-line taken by a particle carrying an electric charge is proportional to the Lorentz force exerted upon it.

From the physical and geometrical point of view, it is an interesting fact that this interpretation of the equations of path is identical with that of general relativity.

Now we will proceed further to consider the track of an electromagnetic wave.

Since the field-equations (3·9) and (3·10) involve only the gravitational potentials $g_{\lambda\mu}$ and the electromagnetic field-tensor $F_{\lambda\mu}$, with their derivatives, but not the electromagnetic potential-vector φ_{ν} explicitly, there exists an arbitrariness of φ_{ν}.

It is usual to avoid this arbitrariness of φ_{ν} by imposing the condition

$$\mathring{\nabla}_{\nu} \varphi^{\nu} = 0. \tag{5·8}$$

By means of equation (5·8), (3·10) is reducible to the form

$$g_{\alpha\beta} \frac{\partial^2 \varphi_{\nu}}{\partial x^{\alpha} \partial x^{\beta}} + (\text{terms not involving second derivatives of the } \varphi\text{'s}) = 0. \tag{5·9}$$

On the other hand, following Hadamard[1], Vessiot[2], de Donder[3] and Whittaker[4], we know that a ray for a wave is identical with the bicharacteristic of the partial differential equations of the second order which represent the wave. Hence, from (5·9), we have

$$\left.\begin{aligned} &\frac{d^2 x^{\nu}}{dt^2} + \left\{ \begin{matrix} \nu \\ \alpha\beta \end{matrix} \right\} \frac{dx^{\alpha}}{dt} \frac{dx^{\beta}}{dt} = 0, \\ &ds = 0, \end{aligned}\right\} \tag{5·10}$$

for the differential equations of the bicharacteristics of (5·9). Consequently we see, from the description in § 2, that this track of a light ray is nothing less than a minimal geodesic in our connection.

Thus we have seen that all the results obtained by the theory of general relativity (with the Maxwell-Lorentz theory) are unified

1. J. Hadamard: Leçon sur la propagation des Ondes (1903), Chap. VII.
2. E. Vessiot: Com. Rend., **166**, 349 (1918)
3. de Donder: La gravifique einsteinnienne (1921), § 29, § 45
4. E. T. Whittaker: Proc. Camb. Phil. Soc., **24**, 32 (1928)

geometrically and physically in a simple form by using a semi-symmetric and metric connection.

In conclusion the writer wishes to express his most cordial thanks to Prof. Tamaki by whose kind advice this work was accomplished.

Experimental Studies on the Sound of A Japanese Hanging Fire-Bell

By

Ichiro Aoki

(Received July 11, 1931)

Abstract

The present paper describes the experimental investigation of the tone colour of a small Japanese hanging bell. The sounds were recorded by a Low-Hilger audiometer, and the curves obtained were analysed by the method of periodogram-analysis. Generally speaking, the sound of the bell used in the experiment contains about five partial tones, and the ratios of their amplitudes change as the time passes after it is struck.

§ 1. Introduction.

The nature of the sound of European church-bells has been studied by many physicists[1]. But so far as the writer knows that of Japanese bells has not yet been studied. The temple-bells in Japan and China are somewhat different from those in Europe in their form and material. Also the method of striking is different. In order to study the nature of the sound of Japanese bells, the writer took a miniature temple-bell, which is now used for the announcement of the opening of temple ceremonies and formerly was used as a fire-alarm too, as the object of his preliminary investigation.

§ 2. The structure of the bell.

A photograph of the bell used in this experiment and its vertical

1. J. Biehle: Archiv f. Musikwiss., 1ster Jahrg., 289 (1919)
J. Biehle: Die Bewertung der Bronze und Gussstahlglocken (1918)
J. Biehle: Phys. Zeits., **22**, 337 (1921)
A. T. Johnes: Phys. Rev., **16**, 247 (1920)
A. T. Johnes: Phys. Rev., **31**, 1092 (1928)
F. G. Tyzzer: Journal of Franklin Institute, **210**, 55 (1930)

cross-section with dimensions are shown in Fig. 1 and Fig. 2.

Fig. 1

Fig. 2

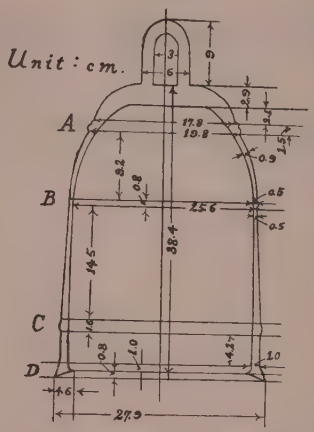

The upper part AB of the bell is usually called "Ibonomachi (studded portion)", as it has many studs on its outer side for ornamentation. The meridian section of this part, as seen in Fig. 1, consists of two circular arcs. But as their centres are not on the axis of the bell, its surface is not spherical.

The middle part BC of the bell is called "Ikenomachi (pond portion)". This part is rather thin and its surface is nearly vertical, the thickness decreasing gradually from the mouth to this point. It is said that this part must be made as thin as possible, but not so much so that the bell will break when it is struck.

The lowest part CD is called "Kusanomachi (grass portion)", and is also nearly vertical and cylindrical like the middle part. But this portion is made thicker and its lowest edge particularly is made very thick. In the case of a large temple-bell, the centre of mass is situated a little above the dividing line between Ikenomachi and Kusanomachi.

There is a belt-shaped thick part between Ikenomachi and Kusanomachi on the outside, having two small circular flat projections on its opposite sides, which are called "Tsukiza (striking seat)". Either of these flat projections is struck with a heavy wooden clapper from the outside to ring the bell.

The total weight of the bell examined is 19 kg., the calibre is 28 cm., and its height is nearly 40 cm. The bell is composed of copper and zinc in the ratio Cu 10 : Zn 1.5.

§ 3. Apparatus.

We used for this experiment a Low-Hilger audiometer. This instrument is often said to have the fault that there is a resonance effect in its diaphragm. We examined it with tuning forks, however, and found that this effect was tolerably small in the frequencies under this investigation.

§ 4. Experimental data.

By striking one of the Tsukiza marked o in Fig. 3, we obtained the photograph shown in Pl. I. This plate shows the variation of the wave-form as the time passed after the striking.

Pl. II, Fig. 1—Fig. 6 show the wave-forms obtained by striking different positions on the belt-shaped part $(90/4)^\circ$ from each other, marked 2, 3 and 4 in Fig. 3. The number of plates and figures, the points struck and the lapse of time between the beginning of the curves and the striking of the bell are shown in the annexed table and Fig. 3.

	Point struck	Time elapsed	
Plate I, Fig. 1	o	o sec.	not analysed
„ Fig. 2	o	0.3 sec.	analysed
„ Fig. 3	o	0.5 sec.	„
„ Fig. 4	o	1.0 sec.	„
„ Fig. 5	o	1.5 sec.	„
„ Fig. 6	o	3.0 sec.	„
Plate II, Fig. 1	1	1.0 sec.	analysed at two parts
„ Fig. 2	1	1.5 sec.	not analysed
„ Fig. 3	1	3.0 sec.	„
„ Fig. 4	2	1.5 sec.	analysed
„ Fig. 5	3	1.5 sec.	analysed at two parts
„ Fig. 6	4	0.5 sec.	analysed
„ Fig. 7	*a*	1.0 sec.	analysed
„ Fig. 8	*a*	1.5 sec.	not analysed
„ Fig. 9	*b*	1.0 sec.	analysed
„ Fig. 10	*b*	1.5 sec.	not analysed
„ Fig. 11	*c*	1.0 sec.	analysed
„ Fig. 12	*c*	1.5 sec.	not analysed

In some of these photographs, we find beats. It can easily be supposed that these beats are caused by the existence of the two "Tsukiza", which act as additional masses to the body.

Fig. 3

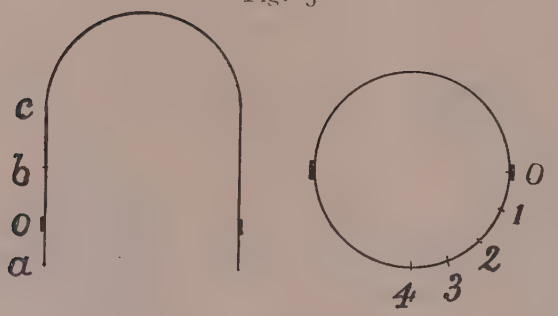

Pl. II, Fig. 7—Fig. 8 were obtained by striking different parts along the meridian which contains the "Tsukiza". The centre of mass of the bell is situated on the horizontal line passing through *B* in Fig. 2.

Fig. 1—Fig. 6 in Pl. I were obtained by changing the interval between the striking of the "Tsukiza" and the opening of the shutter. In these plates, we see that the frequencies of the partial tones do not change, but only the ratios of their amplitudes change, and the same wave-form is repeated every 39 fundamental waves, as shown by *a*, *b*, *c* in the plates.

§ 5. Method of analysing.

Since, as is well known, the component-frequencies of the vibrations of a bell are not harmonic, we can not apply the ordinary method of Fourier's analysis to our curves to get their component sine-curves. Therefore we used the periodogram analysis[1]. Having found one period and its amplitude, we can draw a sine-curve with the period and amplitude found. Then subtracting this curve from the original one, we get a new curve. With this new curve we find another period and its frequency. Continuing this process, we can find the remaining components. This method is very tedious and the result thus obtained is naturally not so accurate as those that can be obtained by the ordinary Fourier method.

§ 6. Results.

The results of the periodogram analysis are shown in the following diagram.

The conclusions obtained from these results are as follows:

1. Whittaker and Robinson: "The calculus of observations". pp. 343-360. Carse and Shearer: Edinburgh Mathematical Tracts. No. 4.

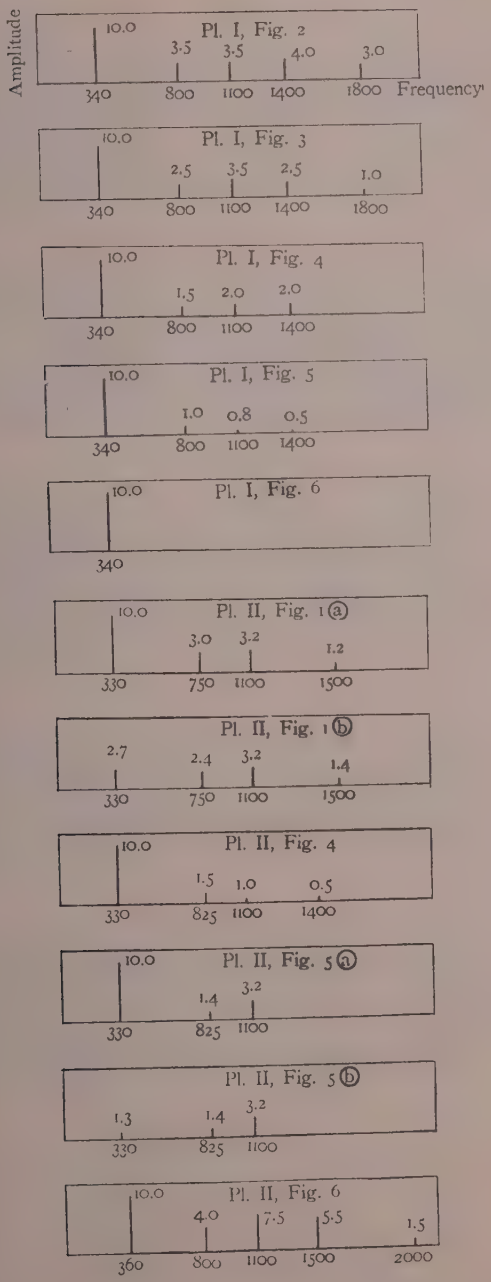
Amplitude
Pl. I, Fig. 2
10.0
3.5
3.5
4.0
3.0
340
800
1100
1400
1800
Frequency
Pl. I, Fig. 3
10.0
2.5
3.5
2.5
1.0
340
800
1100
1400
1800
Pl. I, Fig. 4
10.0
1.5
2.0
2.0
340
800
1100
1400
Pl. I, Fig. 5
10.0
1.0
0.8
0.5
340
800
1100
1400
Pl. I, Fig. 6
10.0
340
Pl. II, Fig. 1 ⓐ
10.0
3.0
3.2
1.2
330
750
1100
1500
Pl. II, Fig. 1 ⓑ
2.7
2.4
3.2
1.4
330
750
1100
1500
Pl. II, Fig. 4
10.0
1.5
1.0
0.5
330
825
1100
1400
Pl. II, Fig. 5 ⓐ
10.0
1.4
3.2
330
825
1100
Pl. II, Fig. 5 ⓑ
1.3
1.4
3.2
330
825
1100
Pl. II, Fig. 6
10.0
4.0
7.5
5.5
1.5
360
800
1100
1500
2000

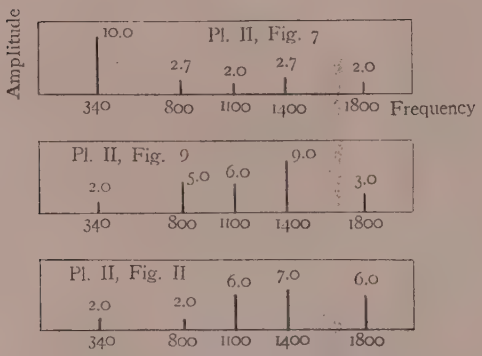

(i) From Pl. I, we see that the fundamental tone (frequency = 340) always has the greatest amplitude. In Fig. 2, the 4th partial (frequency = 1400) has the 2nd greatest amplitude. In Fig. 3 and Fig. 4, the 3rd partial, and in Fig. 5 the 2nd partial has the 2nd greatest amplitude. This shows that among the overtones the highest one predominates immediately after the bell is struck, but it quickly damps away and the next highest one takes its place and so on. And after 3sec., the overtones entirely vanish, and the fundamental tone only continues to exist.

(ii) Pl. II. Fig. 7—Fig. 12 show that higher overtones become intensified as the point struck changes from the lower to the upper part.

(iii) Pl. II. Fig. 1—Fig. 6 show that the beat appears in the fundamental tone as we strike 1 or 3 in Fig. 3. This fact coincides with the classical theory of Helmholtz and Rayleigh.

In conclusion the writer wishes to express his great obligation to Professor Tamaki for his valuable instruction and guidance in this experiment.

Plate I

Fig. 1

Fig. 2

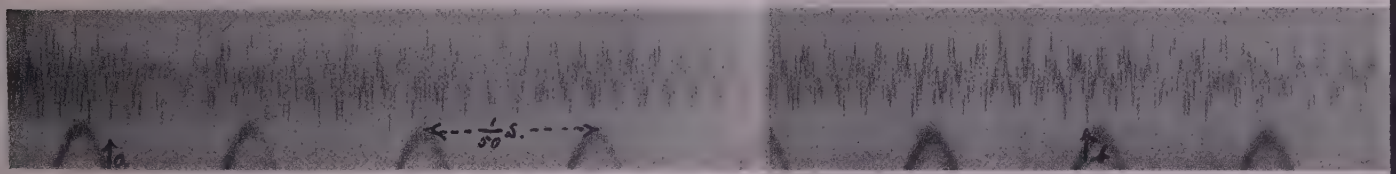

Fig. 3

Fig. 4

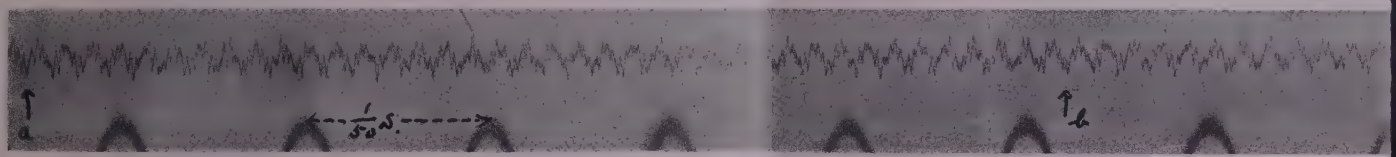

Fig. 5

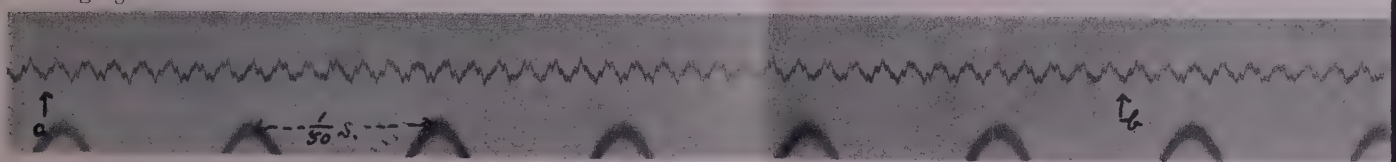

Fig. 6

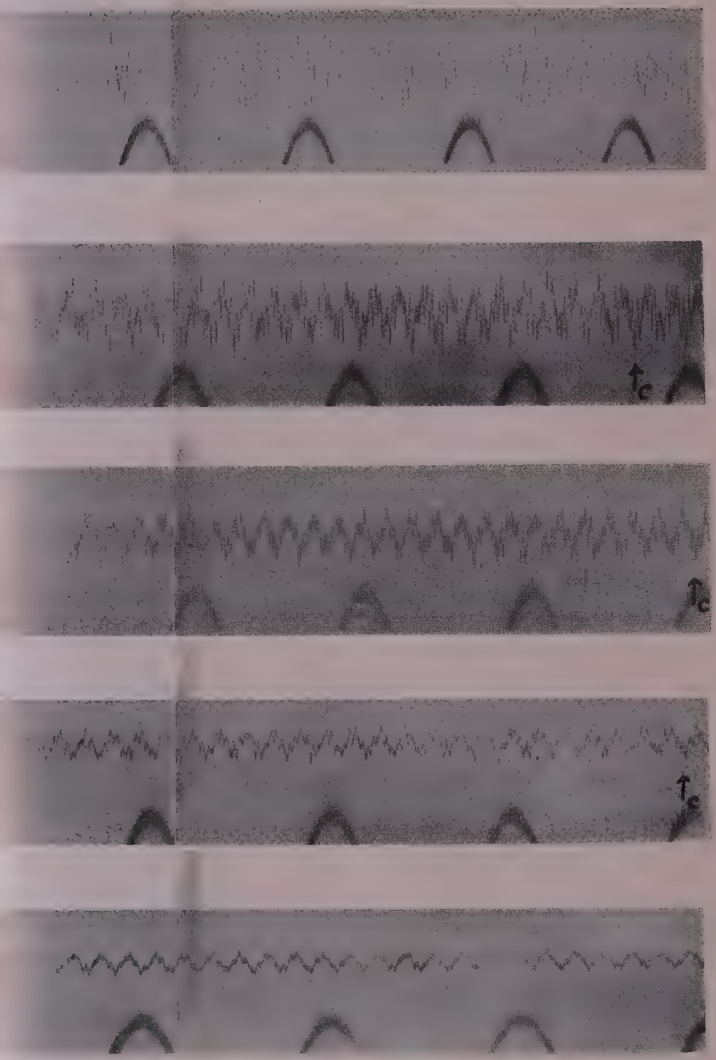
f_c
f_c
f_c

Some Strange Oscillatory Discharge-Figures on Photographic Plates

By

Tatsumi Terada

(Received July 28, 1931)

Abstract

Certain strange discharge-figures are impressed on photographic plates when oscillatory discharges, first negative and then positive, take place at an electrode placed on the plates. The figures thus taken at low air pressures have a strikingly different structure from the ordinary ones obtained with a single discharge, but they are very like those showing the "reversal-like phenomena" which are produced by fogging the photographic plates with a spark simultaneously with the impression of the discharge-figures.

An explanation of these strange oscillatory discharge-figures is given on the same lines as that of the "reversal-like phenomenon."

In an earlier investigation[1] on the discharge-figure impressed on photographic plates, the writer found an interesting positive figure due to the oscillatory discharge of a condenser charged positively, and pointed out a distinct difference between this and the ordinary positive figure. In these interesting positive figures (see Fig. 4 and Fig. 5 in Plate II of that paper), it has been noticed that the figures generally consist of two parts: (1) an indefinite circular part at the centre, from which some short brushes radiate outwards, and (2) some intense branches starting from the centre of the former, from whose ends irregular branches grow outwards and fit themselves in proper order into the space between the brushes of (1). From these features, it seemed to the writer that part (1) was formed by the first discharge at the electrode and part (2) by the next discharge.

In the present paper, we shall investigate the negative figures

1. T. Terada: These Memoirs, **13**, 281 (1930)

Fig. 1

Fig. 2

Fig. 3

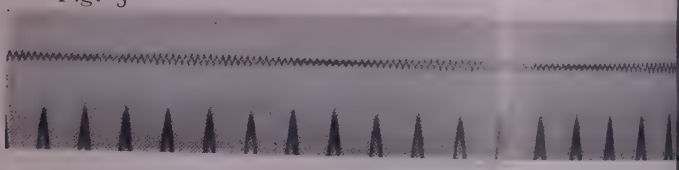

Fig. 4

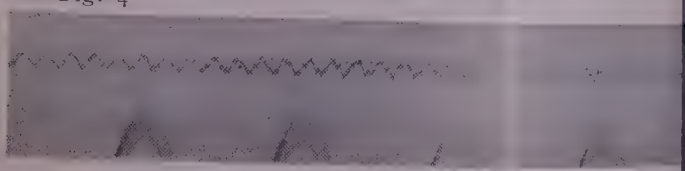

Fig. 5

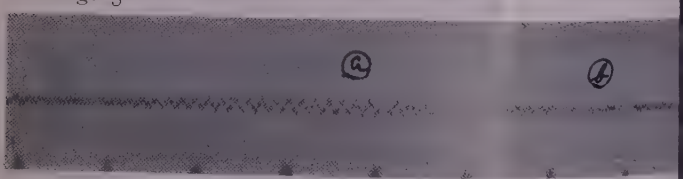

Fig. 6

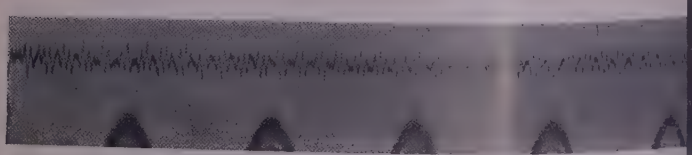

Plate II

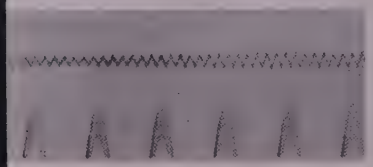

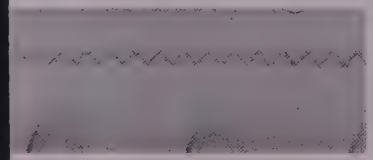

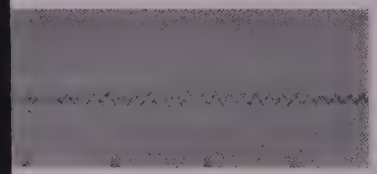

Fig. 7

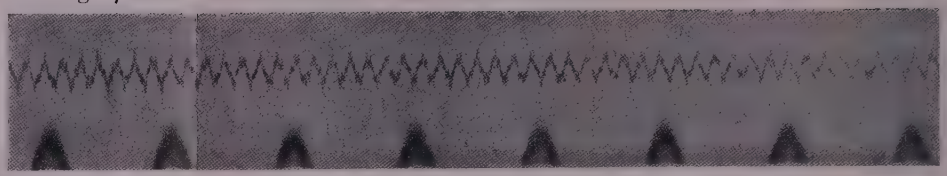

Fig. 8

Fig. 9

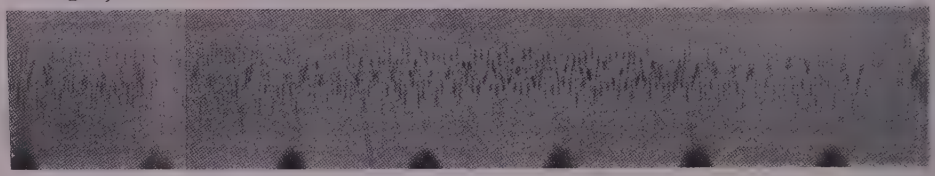

Fig. 10

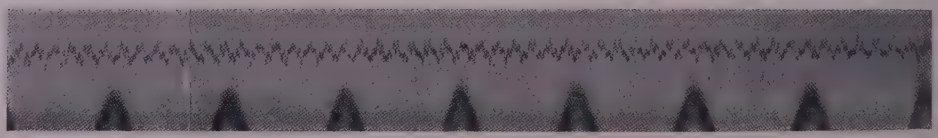

Fig. 11

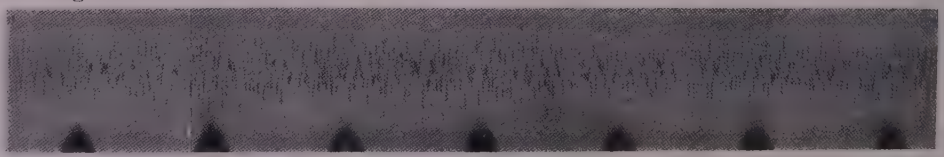

Fig. 12

Some Strange Oscillatory Discharge-Figures on Photographic Plates

By

Tatsumi Terada

(Received July 28, 1931)

Abstract

Certain strange discharge-figures are impressed on photographic plates when oscillatory discharges, first negative and then positive, take place at an electrode placed on the plates. The figures thus taken at low air pressures have a strikingly different structure from the ordinary ones obtained with a single discharge, but they are very like those showing the "reversal-like phenomena" which are produced by fogging the photographic plates with a spark simultaneously with the impression of the discharge-figures.

An explanation of these strange oscillatory discharge-figures is given on the same lines as that of the "reversal-like phenomenon."

In an earlier investigation[1] on the discharge-figure impressed on photographic plates, the writer found an interesting positive figure due to the oscillatory discharge of a condenser charged positively, and pointed out a distinct difference between this and the ordinary positive figure. In these interesting positive figures (see Fig. 4 and Fig. 5 in Plate II of that paper), it has been noticed that the figures generally consist of two parts: (1) an indefinite circular part at the centre, from which some short brushes radiate outwards, and (2) some intense branches starting from the centre of the former, from whose ends irregular branches grow outwards and fit themselves in proper order into the space between the brushes of (1). From these features, it seemed to the writer that part (1) was formed by the first discharge at the electrode and part (2) by the next discharge.

In the present paper, we shall investigate the negative figures

1. T. Terada: These Memoirs, **13**, 281 (1930)

which are obtained with similar experimental arrangements, but which are due to the oscillatory discharge of a condenser negatively charged.

(I) The Figures obtained with an Oscillatory Circuit consisting of an Inductance and a Capacity

The letters used in Fig. 1 have the same significance as in Fig. 3 of the earlier paper; namely, I is an induction coil or an influence

Fig. 1.

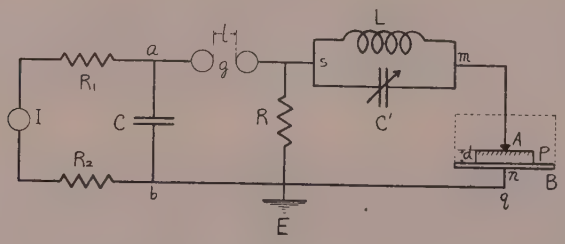

machine, R_1 and R_2 great resistances, R another resistance, L an inductance, C a condenser of about 4,000 cms., C′ a variable air condenser, and P is a photographic plate placed on an earthed metal plate B. The photographic plate P is enclosed, with an electrode A laid on it, in a sealed bell-jar provided with an exhaust arrangement.

In order to get undamped electrical oscillation in the branched circuit (L–C′), it is necessary to use a greater shunt resistance R and a smaller electrode A, because the logarithmic decrement of the circuit depends upon the energy-loss transferred during the periodic time, and among the causes of the losses of electric energy, those due to the shunt resistance and the formation of the figure are especially predominant in our case. Fig. 1 in Plate I is a negative figure obtained with the spark gap $l = 1$ mm. and the shunt resistance $R = 1$ megohm, and at a low air pressure of about 120 mm. Hg. The wave-length λ of the oscillation in our branched circuit could be measured by means of a wave-meter by passing sparks successively at the gap g, though the oscillation was not strong. In our case it was about 100 meters. Generally speaking, this figure consists of two parts: namely, (1) a central diffuse portion from whose center well-known irregular positive branches start outwards, (2) a continuous margin just at the end of the former, leaving a narrow dark unaffected portion between this

margin and part (1).

Next, in order to get the negative discharge-figure which will be impressed on a photographic plate when many oscillatory discharges occur at the electrode, the thickness d of the insulating plate was increased to 2 mm. or more to reduce the energy-loss on the formation of a figure. Fig. 2 in Plate I was obtained with $d=2$ mm., $l=1.2$ mm., air pressure $p=150$ mm. Hg, R = 1 megohm and $\lambda=25{,}000$ m. In this, we can see two negative enveloping rings similar to that in Fig. 1 in the same plate and also many positive branches radiating from the electrode. Some of the positive branches appearing near the electrode seemed to differ a little from the ordinary ones: their side portions were a little stronger in intensity than the inside, though this might not be clearly reproduced.

In order to make clearer the features of such positive branches, many photographs were next taken with other oscillatory circuits in which the oscillations were a little longer and stronger than in the former cases.

(II) The Figure obtained by an Oscillatory Circuit with a Low-pressure Discharge-tube

As many observers[1] have noticed, it is possible to generate electric oscillations with an audio or radio frequency by the aid of a discharge-tube containing gas at low pressure. In Fig. 2, I, R_1, R_2, C, g, A, P, B and L have the same significance as in Fig. 1. V is a discharge-

Fig. 2.

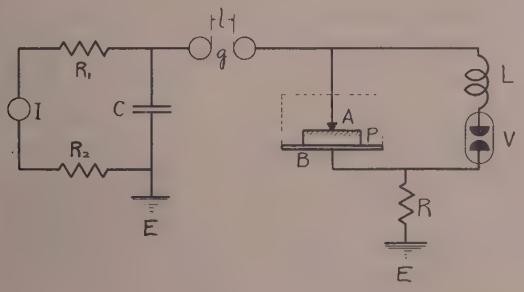

1. R. Bär: Handbuch der Physik, (Geiger und Scheel) XIV, 178 (1927)
K. G. Emeléus: The conduction of electricity through gases, 19 (1929)
E. W. B. Gill: Phil. Mag. **8**, 955 (1929)

tube with aluminium electrodes whose air pressures were generally below a few millimetres of mercury but varied within wide limits. If, as the right hand-side in the figure makes an oscillatory circuit, direct current-discharges pass through the gas in tube V, oscillations will occur in the circuit ALVBA and consequently the discharges-negative and then positive- will take place at the electrode A several times. The wave thus obtained may also be of sinusoidal form as is often the case with oscillations produced by a discharge-tube. However, the wave-length of the oscillation in this case could be easily measured by means of the precision wave-meter, for the oscillation was stronger than in the former cases.

Fig. 3 in Plate I was obtained with such an experimental arrangement; that is to say, the condenser C was negatively charged and $l = 1.3$ mm., $d = 2.5$ mm., $R = 3{,}400$ ohms, $p = 65$ mm. Hg, and $\lambda = 1{,}800$ m. From this, as we expected, it seems that the oscillations lasted for a comparatively long time and consequently three or more negative and two or more positive discharges occurred at the electrode one after another. In this figure, there are two or more concentric rings which are essentially the same as the enveloping margin in Fig. 1 or those in Fig. 2 in the same plate, though they are rather too faint to give a clear reproduction. And also, we can distinctly see two kinds of positive branches in this; namely (1) the ordinary positive branches which were perhaps due to the first positive discharge, (2) peculiar positive branches as if a photographic reversal had taken place, which were probably impressed on the photographic plate by the second positive discharge (i. e. this was preceded by the first negative and positive and the second negative discharges).

To establish the relations between the occurrence of these strange phenomena and the periodic time of the discharges at the electrode, many photographs were made with oscillatory circuits with various periodic times. By changing the air pressure in the discharge-tube or the inductance L, the wave-lengths were varied between very wide limits from 60 to 25,000 meters or more, and the experimental results suggested that the occurrence of the phenomena would be nearly independent of the periodic time of oscillations produced in the circuits so long as the oscillatory discharges occurred at the electrode.

(III) An Explanation of the Strange Oscillatory Discharge-Figures

In Fig. 3, A, P and B have exactly the same meaning as in the previous figures. G is a spark gap inserted between the electrode A and the earthed metal plate B. If a discharge-figure—positive or negative—is impressed on the photographic plate P, and at the same time a fogging spark passes over the gap G, an interesting phenomenon occurs in the figure as Prof. U. Yoshida[1] first pointed out. In the negative, a diffuse enveloping margin appears just at the ends of the regular negative branches, leaving a nearly unaffected narrow area between them (see Fig. 4 in Plate I). In the positive, each branch is enveloped by a rather diffuse margin (see Fig. 5 in the same plate). The writer will call this the "reversal-like phenomenon" as in his earlier paper[2].

Fig. 3

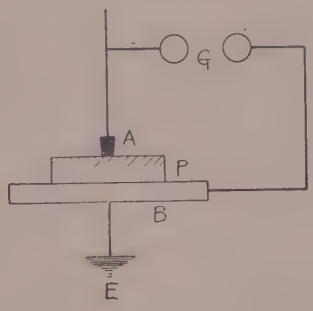

In that paper, the writer tried to give an explanation of the occurrence of the phenomenon from the facts: (1) the wave-length of the fogging light which was effective in the phenomenon was shorter than about 420 $\mu\mu$ as pointed out by Prof. U. Yoshida and J. Tsutsumi[3], (2) the features of the figures showing these phenomena were very like those of dust-figures, and (3) similar phenomena occurred in the discharge-figures impressed on photographic plates which had been previously charged with electricity in some way though they were too faint to be reproduced in that paper.

Now, comparing the features of the enveloping margins of the strange oscillatory figures with those showing the "reversal-like phenomena"—compare Fig. 1 with Fig. 4 in Plate I and also Fig. 3 with Fig. 5 in the same plate—, it seems probable that these phenomena are due to the same causes.

Let us assume that, in Fig. 4, the greater circle denotes the range of the first negative figure. Just after the impression of this,

1. U. Yoshida: These Memoirs **2**, 315 (1917)
2. T. Terada: These Memoirs **12**, 217 (1929)
3. U. Yoshida and J. Tsutsumi: These Memoirs **11**, 267 (1928)

Fig. 4

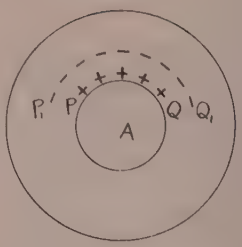

numerous negative ions and some positive ions will be left within the range and their number may be increased by the following positive discharge at the electrode A. If at this stage, the second negative discharge-figure is impressed on the plate and its range is denoted by the smaller circle in Fig. 4, the positive ions thus produced on the plate will be attracted inwards and left in a layer PQ just at the edge of the second negative, but numerous negative ions or electrons will be repelled outwards and crowd in the other layer P_1Q_1 in the manner shown in Fig. 4. As this will bring forth a weak electric field in the portion between the layers PQ and P_1Q_1 and a strong field in the layer P_1Q_1 or a little outside it, the negative enveloping margin will be formed in that portion where the strong field is, as a result of ionization caused by collision of the ions with air molecules, and will miss the unaffected dark ring at the weak portion of the field between the layers PQ and P_1Q_1 as stated in the writer's earlier paper in the explanation of the "reversal-like phenomenon." Thus, the negative enveloping margin of Fig. 1 in Plate I may be produced. From this point of view, it follows that if several negative discharges caused by an oscillatory circuit take place at an electrode placed on a photographic plate, the phenomena mentioned above should occur for successive pairs of them. The diffuse concentric rings in Fig. 2 in Plate I were probably produced in this manner.

If there is no great mistake in this explanation, we should also be able to get similar figures by other methods which can cause successive negative discharges at an electrode placed on a photographic plate. This was found to be true: similar figures have been obtained on dried photographic plates at low air pressures when two or more negative discharge-figures were successively impressed, within a few seconds, the ordinary arrangement being used, but they were a little too faint to be reproduced.

It seems to the writer that the enveloping margin of the positive branches in the oscillatory figure (Fig. 3 in Plate I) is essentially the same as the negative margin in Fig. 1 in the same plate and consequently the explanation given above is also applicable to the positive. The main difference between them seems to be only the arrangement

of the branches, but it is hardly necessary to mention the point, for it was fully described in the earlier paper[1]. The only question left to be explained is why the positive branches, which were impressed after the first negative, are not enveloped by the margin (i. e. we can not see the enveloping margin in the positive branches in Fig. 1, Plate I). This may be simply that the number of ions, especially the positive ions, was insufficient to make the portions of the weak and the strong electric field distinct and consequently, the enveloping margin was not produced in the positive branches in Fig. 1, Plate I.

In a word, the main result of the investigations mentioned hitherto is that the strange oscillatory figures are none other than those giving rise to the "reversal-like phenomena" and that both the previous discharges of the oscillatory figure and the fogging spark in the "reversal-like phenomenon" have the same influence upon the positive and negative figures in question.

In conclusion the writer's sincere thanks are due to Prof. U. Yoshida of the Kyoto Imperial University for the interest he has taken on the research.

1. T. Terada: loc. cit. (1929)

Plate I

Fig. 1

l=1mm. d=1.2mm. R=1 meg.
λ=100m. p=120mm. *Hg*.

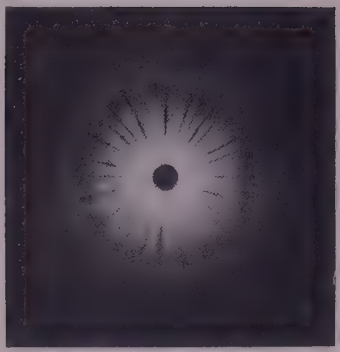

Fig. 2

l=1.2mm. d=2mm. R=1 meg.
λ=25,000m. p=150mm. *Hg*.

Fig. 3

l=1.3mm. d=2.5mm. R=3,400 ohms.
λ=1,800m. p=65 mm. *Hg*.

Fig. 4

l=2.5mm. p=760mm. *Hg*.

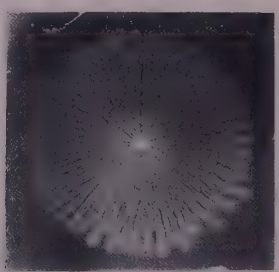

Fig. 5

l=2.5mm. p=760mm. *Hg*.

X-Ray Diagram Lines Strongly Absorbed in the Absorption Spectra

By

Suekichi Kawata

(Received August 7, 1931)

Abstract

Continuing his research on the origin of the X-ray absorption edge, the author adopted the method of determining the relative position of the emission line and the corresponding absorption limit from the diminution of the intensity of the line passing through an absorbing screen of the same element. It was found that (1) $L\beta_5$ lines of W and Pt were strongly absorbed, (2) the Au $L\beta_5$ line was absorbed somewhat more than other lines on the longer wave-length side of the edge, and (3) the Cu $K\beta_2$ and the Pt $L\gamma_6$ lines were only slightly absorbed. From these results an explanation of the origin of the absorption limit is propounded.

In the previous research on the relation between the K absorption edge and the $K\beta_3$ line of Ni, Cu and Zn[1] the author found that in the case of Cu the line and the absorption limit fell so near each other that it was impossible to decide which was on the shorter wave-length side. The object in the present investigation was to elucidate this relationship from the intensity of the emission line absorbed by a screen of the same element. For this purpose the author used a copper anticathode, on which a small amount of zinc was electrically deposited, and a copper absorbing foil with a mass of 13 milligrams per square centimeter. The spectrograms were taken on two different horizontal portions of the same plate, one corresponding to the case where the absorber was used, and the other to the case where it was not used. The exposure was carried out for the two portions alternately several times. The time of exposure was so adjusted as to give a slightly stronger intensity for the portion with the absorber on the longer wave-length side of the absorption limit. Thus from the comparison of the two parts on the plate it was easily concluded that

1. S. Kawata: These Memoirs, 14, 55 (1931)

also in the case of Cu the $K\beta_2$ line is located on the longer wave-length side of the K absorption limit[1]. This method is due to Walter[2]. He used the method for the determination of the absorption edges of Ni and Zn, but the author found it very effective especially for such an investigation as the present.

Recently Sandström[3] has reported some interesting results drawn from the measurements made by himself and some other investigators. According to these results the $L\gamma_6$ lines of Ta, Re and Ir are of shorter wave-lengths than the L_{II} limits, and the $L\beta_5$ lines of W, Re, Ir and Pt of shorter wave-lengths than the L_{III} limits, and this will be of great importance for the knowledge of the origin of the absorption limit[4]. But it seemed to the author from his experience in connection with the K limit and the $K\beta_2$ line that some ambiguity must accompany such delicate results when the data are obtained from the comparator readings, especially those of different investigators. He therefore undertook the task of ascertaining the existence of such lines of wave-lengths which coincide with or are shorter than the absorption limit, using the above mentioned method.

The experiment was carried out for W $L\beta_2$, Pt $L\beta_5$, $L\gamma_6$ and Au $L\beta_5$. In the case of Pt and Au a rolled foil of each metal weighing 20 milligrams per square centimeter was used, while in the case of W the metallic powder mixed with Zaponlack and spread upon a filter paper to the mass of 18 milligrams per square centimeter was used.

The results were that (1) W $L\beta_5$ and Pt $L\beta_5$ were distinctly absorbed, (2) Pt $L\gamma_6$[5] was only slightly absorbed and (3) Au $L\beta_5$ was absorbed somewhat more than the other lines on the longer wave-length side of the limit but not so much as the W and Pt $L\beta_5$ lines.

Thus, it may be concluded that (1) the L_{III} limits of W and Pt correspond to the transition from L_{III} to O_V, (2)[5] L_{II} of Pt corresponds to the transition from L_{II} to the level outside the O_{IV} and (3) Au L_{III} electrons may sometimes stop at $O_{IV, V}$.

In conclusion, the author wishes to express his cordial thanks to Prof. Ishino for his kind guidance throughout the research.

1. It must be noticed, however, that the relation between the $K\beta_2$ line and the K limit is different for the elements Ni, Cu and Zn, as mentioned in the former paper.
2. B. Walter: Zeits. f. Phys., 30, 350 (1924).
3. A. Sandström: Zeits. f. Phys., 66, 784 (1930).
4. Cf. M. Siegbahn: Zeits. f. Phys., 67, 567 (1931).
5. In reality the expression "Pt $L\gamma_6$ line" is not adequate in this case, because that line appears on the photographic plate only as a superposition of the $L\gamma_6$ and $L\gamma_2$ lines, and so conclusion (2) may be somewhat ambiguous, though it seems highly probable that it is correct.

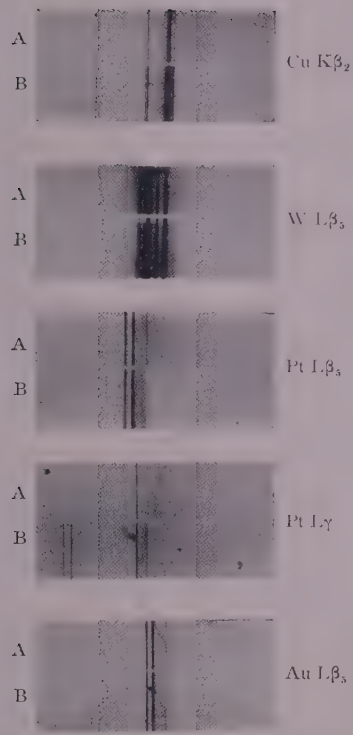

A : Spectrum without the absorber.
B : Spectrum with the absorber.

On the Multiple Structure in the *K* X-ray Absorption Spectra of the Metallic Elements Cr, Mn, Fe, Co, Ni and Cu

By

Masao Sawada

(Received August 7, 1931)

Abstract

An extended multiple structure of the *K* X-ray absorption spectra of the metallic elements Cr, Mn, Co, Fe, Ni and Cu has been photographed.

Some of them extend over an energy range of more than 400 volts.

Throughout the work, the absorbing media were pure metallic elements.

They were prepared by the method of electrodeposition and in the case of manganese the evaporation method was chosen, with a specially designed apparatus.

For copper, in addition to the plates taken with an extra metallic screen, a single-crystal of copper served as the analyser and also as the absorber.

The spectrograms and the microphotometer curves of them are shown.

Several views to account for the origin of the extended multiple structure have been proposed by investigators, but here two hypotheses were taken into consideration and compared with the experimental data.

The first hypothesis considered was that of multiple electron transitions due to the absorption of a quantum of X-rays.

The second was that of the ejection of a *K*-electron from the multiply ionized atom in various shells.

In accordance with the first hypothesis, the energy level diagram for multiple X-ray ionization was constructed on the assumption that the $\{jj\}$ coupling of electrons holds. The intersections of the curves of multiple ionization of different degree are interesting compared with the experimental curves. Of course some discrepancies between the calculated and observed value may be expected owing to the change in electron coupling from $\{jj\}$ to $\{LS\}$. This point is discussed, use being made of the recently published results of S. Goudsmit.

In accordance with the second hypothesis, some calculations were made by extending Wentzel's work. The experimental fact that the slow change of the vaule of $\frac{\nu}{R}$ with the atomic number of the corresponding lines of similar intensity and structure are favourable to this view. But there remains a theoretical question of the new quantum mechanics as to which of the processes suggested by the two hypotheses most frequently occurs.

As a whole, the most probable explanation seems to be that two such phenomena occur in the process of absorption of X-rays.

Introduction

DURING the last few years a very complicated, "fine structure" or "multiple structure" of the short wave-length side of the edge of the X-ray absorption spectra has been investigated.

In an investigation of the absorption spectra of calcium, using a crystal containing the element both as a diffracting crystal and as an absorbing medium, Lindsay and Van Dyke[1] obtained four secondary edges.

But the explanation of this was not satisfactory. In the case of elements of low atomic number, the valency of the element affects the position of the absorption edge, and we have no sure knowledge of the terms of lower levels. In consideration of this, I chose a copper single-crystal[2] as an analyser and an absorber, and obtained as many as five secondary edges, as shown in Fig. 2 (A) (Plate), and put forward the explanation[3] that these were the absorption edges corresponding to the simultaneous removal of the K and M electrons of copper. At about the same time, Nuttal[4] got similar results for potassium and chlorine in chemical compounds.

Later, many researches were made in the same direction.

For example;

Lindsay and Voorhees[5] (Iron: metallic element, and many of its chemical compounds)

Meyer[6] (Bromine: Bromate)

Coster[7] (Copper: metallic element)

Lindh[8] (Copper and nickel: metallic element)

Recently B. Kievit, and G. A. Lindsay[9] obtained many secondary edges for the metallic elements Zn, Cu, Ni, Fe, Co, Cr, and Ca and also for Mn-alloy. And on the basis of multiple ionization the probable transitions of the electrons have been determined to account for them.

---

1. G. A. Lindsay and G. Van Dyke, Phys. Rev. **27**, 508 (1926)
2. This sample was kindly prepared in the laboratory of Prof. Yoshida by Mr. S. Takeyama.
3. M. Sawada, in a paper read at the meeting of our seminary.
4. J. M. Nuttal, Phys. Rev. **31**, 742 (1928)
5. G. A. Lindsay and H. R. Voorhees, Phil. Mag. **6**, 910 (1928)
6. H. T. Meyer, Wiss. Veröff. a. d. Siemens-Konzern VII **2**, 101 (1929)
7. D. Coster, Nature **124**, 652 (1929)
8. A. E. Lindh, Zeits. für Physik, **63**, 106 (1930)
9. B. Kievit and G. A. Lindsay, Phys. Rev. **36**, 648 (1930)

I have studied the same range of elements and their compounds since 1928, and the part of my investigation dealing with the metallic elements from Cu (29) to Cr (24) inclusive will be here described.

Part I. Experimental

(I) The X-ray Apparatus

For obtaining spectrograms of the absorption edges, a Seemann's "edge" vacuum spectrograph was used. The X-ray tube attached to it was a modified large electron tube of Siegbahn type, constructed in this laboratory. A calcite crystal served as a reflector and was continuously rotated through an angle of about 2.5° around the wave-length in question. The current through the tube was about 20 milliamperes, the time of exposure[1] varying from 50 to 100 hours. The voltage applied to the tube was supplied by a large induction coil and was regulated so as to prevent the excitation of second-order emission lines in the region under investigation.

The X-ray tube was evacuated by a Gaede three-stage steel pump, preceded by an oil pump. A thin aluminium foil covered the window of the tube, and separated it from the vacuum spectrograph, which was evacuated by the oil pump alone.

(II) The Preparation of the Absorbing Screens

The problem of obtaining absorbing screens of suitable thickness (thinner than 0.01 m.m.) for the best photographic impression of the multiple structure of the absorption limit is experimentally a difficult matter.

In the investigation here reported they were prepared by the method of electrodeposition or evaporation.

1. Nickel. The solution of electrolyte which was used had the following composition: nickel sulphate 125 gms., ammonium chloride 17 gms., boric acid 15 gms., and water 1000 c.c. This was used at a temperature of about 23°C, with a current density of 0.7 amps. per dm^2. A thin copper plate was immersed in the $K_2Cr_2O_7$ solution, then within quite a short time an imperceptible film of oxide was formed, and this plate was then coated with nickel. Stripping was most likely to occur, and it occurred very markedly.

1. Only 20 hours in the case of copper single-crystal.

2. Cobalt. To a solution of sulphate of cobalt (cryst.) containing 25 gms. of the salt per 50 gms. of water, 0.85 gm. natrium chloride and 2.25 gms. boric acid were added and dissolved. A current density of 1.1 amps. per dm^2 and a temperature ranging from 20° to 25°C was used. The deposit from this solution on a chromium plated copper electrode was very bright, and of a brilliant white colour.

The deposited cobalt film could be stripped from the electrode by heating it gently.

3. Iron. The electrolyte was composed of 600 gms. ferrous chloride and 670 gms. calcium chloride per liter of water. A temperature of about 100°C and a current density of 10 amps. per dm^2. was used.

The anode was of platinum. Iron was deposited on zinc plate and after slightly heating it could be peeled off, yielding smooth, dense films that could be handled without danger of breaking.

4. Chromium. In this case the electrolyte was a solution composed of 200 gms. chromic acid per liter of water used at room temperature with a current density of 50 amps. per dm^2. The method of deposition on copper followed by removal of the copper by dissolving it in dilute nitric acid was only partly successful, the thin film of chromium being broken by the weight of the residual copper itself, on account of the irregular etching of the copper by the acid. The next method tried was one in which a very thin sheet of copper was thinly chromium plated and after rinsing in water, this was again dipped into the copper plating vat, and received over it a thin coating of copper. This was followed by slight annealing and then the copper was dissolved in dilute nitric acid. Finally a very good brilliant chromium screen was obtained.

5. Manganese. The production of uniform manganese screens of the required thickness was difficult. Many attempts were made; (1) by cathodic sputtering, (2) by electrodeposition on Wood's alloy, and so on. Finally the evaporation method was chosen as the best one.

The essential feature of the evaporation method of obtaining a film is the moving of two aluminium foils back and forth one above and the other below an electrically heated filament of the metal under investigation. The particles of metal given off by the hot filament adhere to the foil, giving uniform film. The details of the evaporation apparatus are shown in Fig. 1.

Two sets of two steel rails are fitted into a brass disc and a water-cooled conical brass ground joint. Two brass frames, which can hold an aluminium foil, constitute the carriage. Through the centre

Fig. 1

The evaporation apparatus.

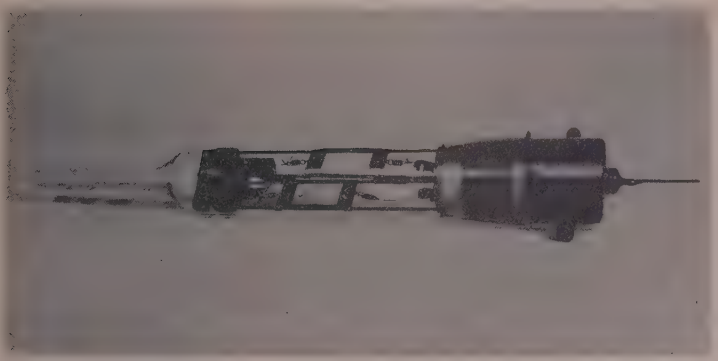

of the conical ground joint, a steel wire protrudes and serves as an electrode and also a holder of a tungsten filament, upon which manganese was coated by electrodeposition[1].

The electromagnet turns around the glass tube. The small piece of iron turns with the magnet. By means of a small capstan, the carriage is drawn along the rails. Thus the carriage moves back and forth along the rails.

The tube was connected to a Gaede three-stage steel pump, with an oil pump as fore-pump. The minimum distance of the wire from the aluminium foil was less than the mean free path of the gas molecules.

Evaporated manganese was found to be very bright and uniform in thickness. This served as an absorber and as a window for the X-ray tube.

(III) Measurements

In measuring the absorption edge of the spectrogram by the comparator the cross hair of a microscope of low magnifying power was brought up to the points where the blackening begins to increase and also to disappear. This was very difficult, and especially for the faint and diffuse edge comparatively large errors might be introduced.

The width of the slit was 0.025 m.m. and no correction due to it was made. The computation of the wave-length of edges or lines was as follows:

1. Handb. d. exp. Phys. Bd. 1, 463 (1926)

Let a be the separation between two reference lines λ_1, and λ_2, and Δa that between the required wave-length λ and λ_2; and let the glancing angle of wave-lengths $\lambda_1, \lambda_2, \lambda$ be $\theta_1, \theta_2, \theta$ respectively; then, we have

$$\tan\theta = \tan\theta_2 - \frac{\Delta a}{a}(\tan\theta_2 - \tan\theta_1).$$

The evaluation of wave-lengths is accomplished by means of Bragg's formula. But in using the preceding formula the reflecting crystal and the X-ray plate must be perpendicular to each other.

(IV) The Microphotometric Records

The curves shown in Figs. 3 (A)–(K) are microphotographs taken with a Moll-microphotometer[1]. They served as the check for the wave-length determination and also for showing general views of the spectrogram. Figs. 3. (C), (E), (G) and (K) were taken with a somewhat narrow slit than the others.

Fig. 3 (A)—(B)

Microphotometric records of the multiple structure in the K absorption spectra.

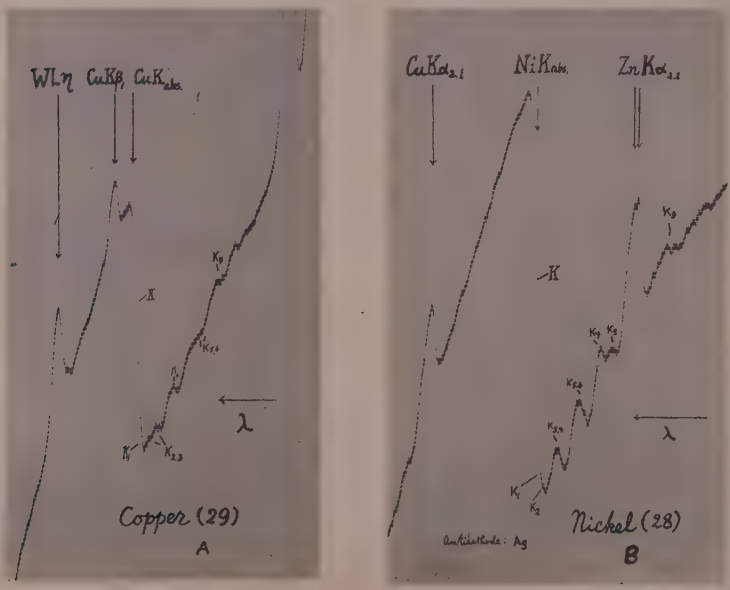

1. The author wishes to express his thanks to Mr. E. Kasai for his kind help in preparing the curves.

Fig. 3 (C)—(E)

Microphotometric records of the multiple structure in the K absorption spectra.

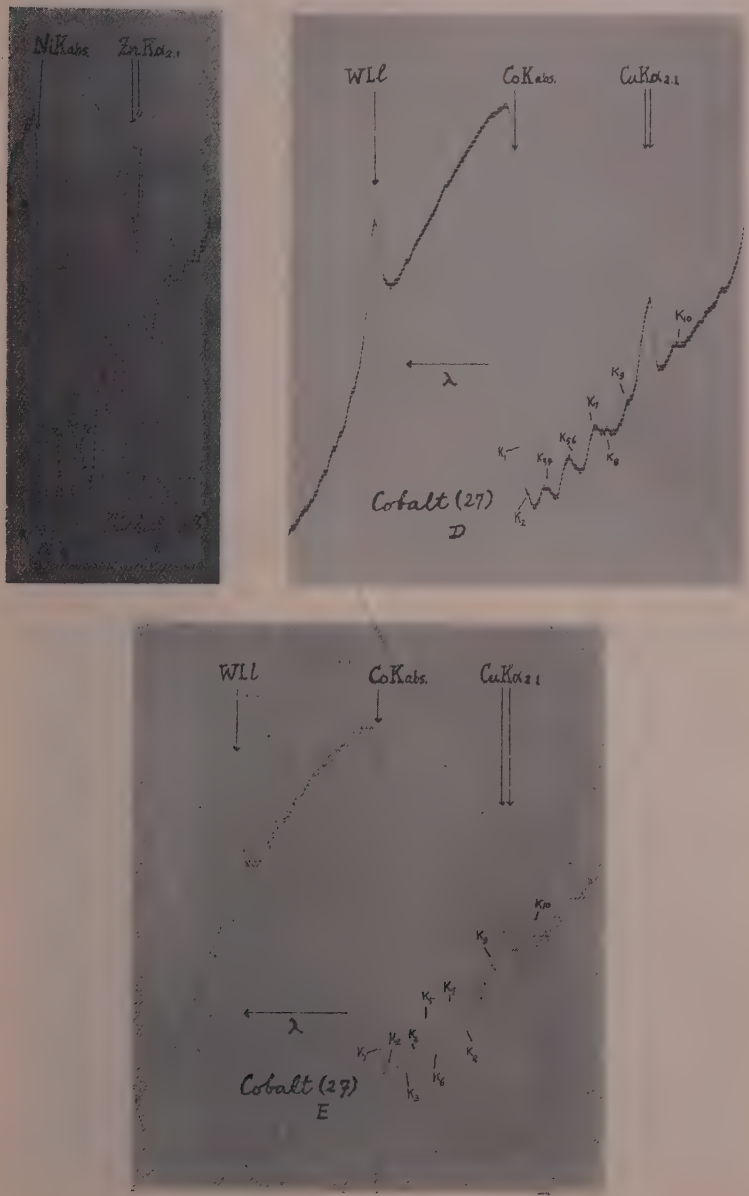

Fig. 3 (F)—(H)

Microphotometric records of the multiple structure in the K absorption spectra.

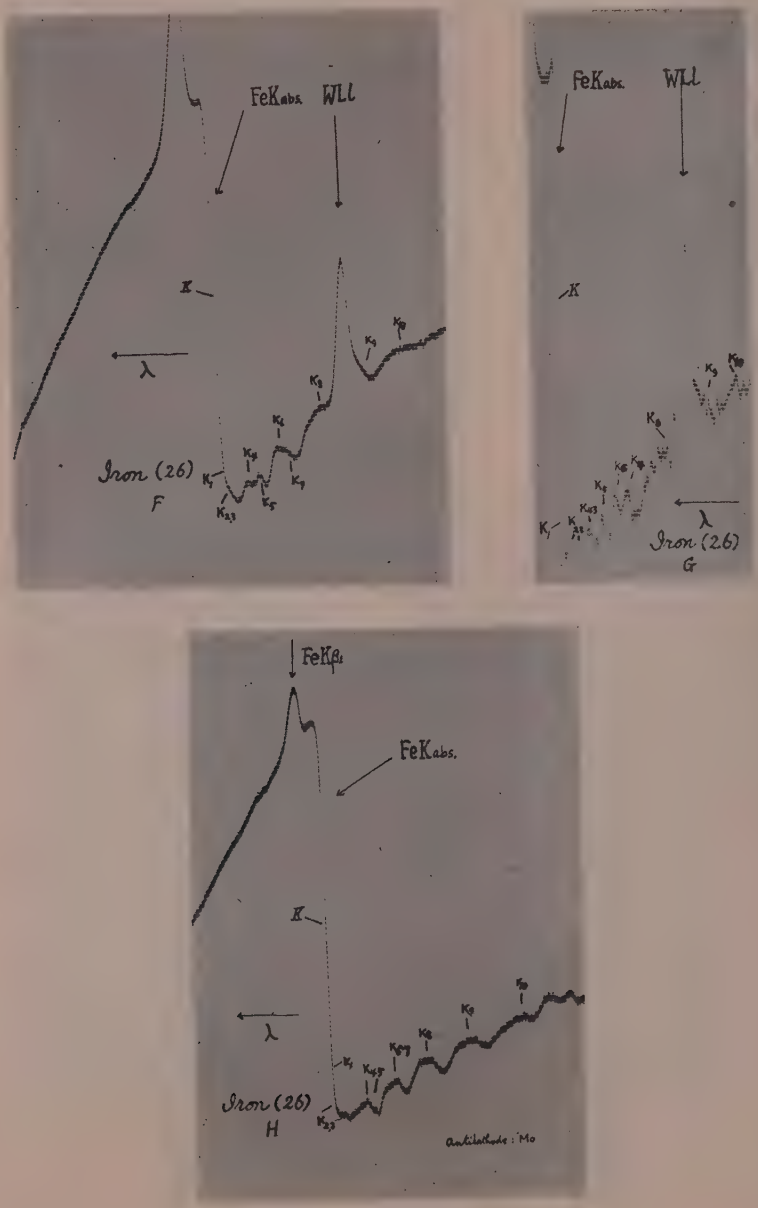

Fig. 3 (I)—(K)

Microphotometric records of the multiple structure in the K absorption spectra.

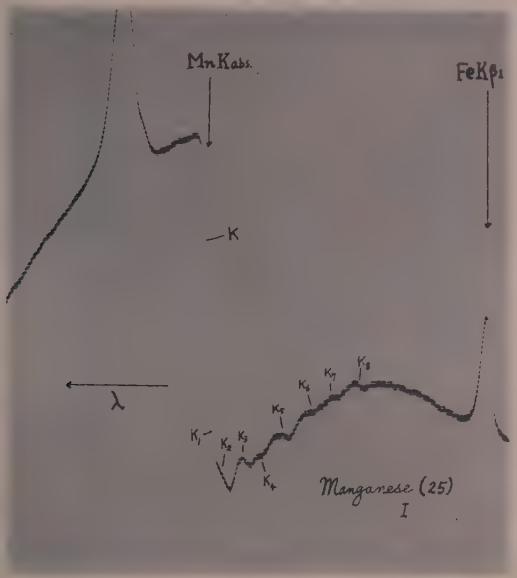

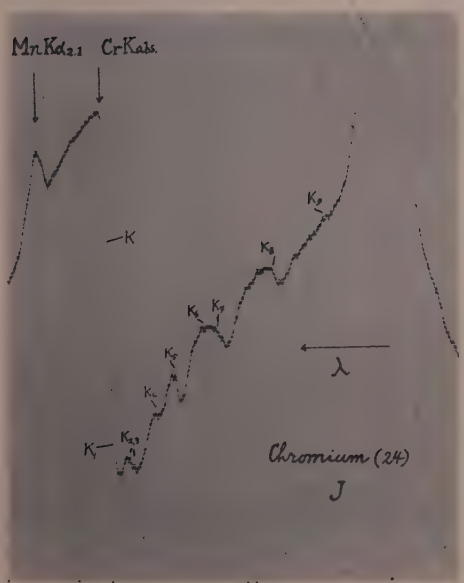

(V) The Spectrograms

Reproduction of the spectrograms are given in Fig. 2 (Plate).

The materials of the anticathode and the cathode and the wave-lengths of the reference lines are given in Table I.

Table I

Spectrogram	Element	Anticathode	Cathode	Reference Lines
Fig. 2 (B)	Cu (29)	Tungsten	Tungsten	$WL\eta$ $\lambda=1418.10$, $WL\beta_1\lambda=1279.17$
„ (C)	Ni (28)	Silver	An oxide-coated platinum filament	$CuK\alpha_2$ $\lambda=1541.16$, $ZnK\alpha_1$ $\lambda=1432.06$
„ (D)	Co (27)	Tungsten	Tungsten	$WL\iota$ $\lambda=1675.00$, $CuK\alpha_1$ $\lambda=1537.26$
„ (E)	Fe (26)	Tungsten	Tungsten	$WL\iota$ $\lambda=1675.00$, $FeK\beta_1$ $\lambda=1753.01$
„ (F)	Fe (26)	Molybdenum	An oxide-coated platinum filament	$CuK\alpha_1$ $\lambda=1537.26$, $FeK\beta_1$ $\lambda=1753.01$
„ (G)	Mn (25)	Tungsten	Tungsten	$FeK\alpha_2$ $\lambda=1932.08$, $FeK\beta_1$ $\lambda=1753.01$
„ (H)	Cr (24)	Tungsten	Tungsten	$MnK\alpha_1$ $\lambda=2097.51$, $FeK\alpha_1$ $\lambda=1932.08$

(VI) Data and Results

The results obtained have been collected in Table II.

The long wave-length side of the white line is denoted by the letter k_l, and the short wave-length side of the same white line by k'_l ($l=1, 2, 3.....$).

The wave-lengths are followed by the values of $\frac{\nu}{R}$ and $\sqrt{\frac{\nu}{R}}$.

In this table may also be found the separation from the principal K-edge, expressed in wave-lengths, in $\frac{\nu}{R}$-units and also in volts.

Here the following physical constants were used.

$$\log 2d = 0.7823347 \qquad (d = 2814.47 \text{ X. U. for calcite})$$

$$\log \frac{\nu}{R} = 5.9596469 - \log \lambda$$

$$V(\text{volts}) = 13.56 \times \Delta\frac{\nu}{R}.$$

From the values of $\Delta\frac{\nu}{R}$ in this table, the curves of Fig. 4 are constructed.

Fig. 4

Diagram of the multiple structure of the K absorption spectra.

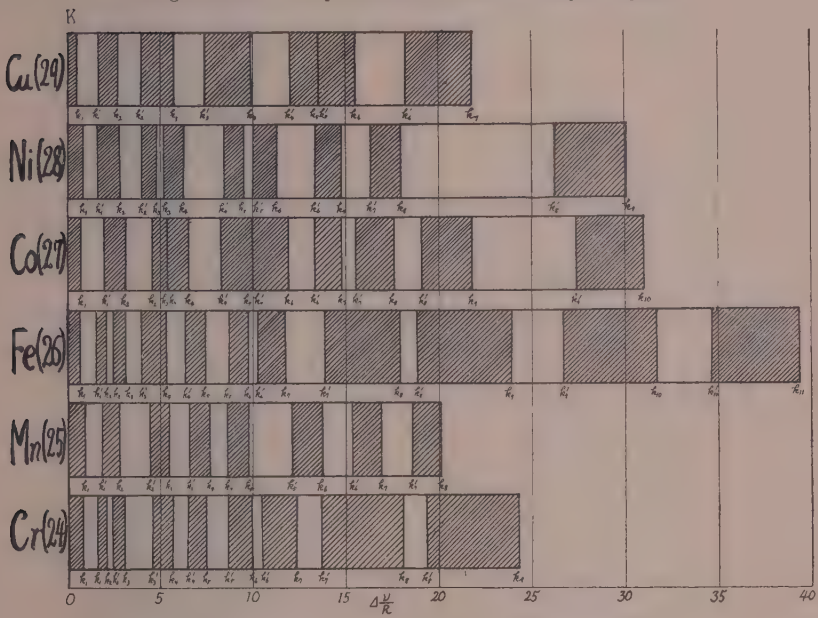

In their general features, the results were nearly the same as those of B. Kievit and Lindsay,[1] although they did not give the results of measurement of the long wave-length side of the multiple structure.

The main new results here obtained are as follows.

I. Nickel (29): Due to the appearance of the Zn$K\alpha_{1,2}$ lines one edge reported by Kievit and Lindsay could not be found. But a new faint edge (k_3) and a fairly strong edge (k_5) were observed.

II. Cobalt (27): The Cu$K\alpha_{1,2}$ radiations were very faint, so more edges (k_9), (k_{10}) were observed than by Kievit and Lindsay. New edges (k_3), (k_5), (k_7) were detected. Besides this plate, using a cobalt screen made by pouring a mixture of powdered cobalt and zapon enamel on a glass plate, two spectrograms were taken. The white lines given by this plate were narrower than those obtained with the metallic sheets. The main edge was very sharp. These changes might be ascribed to the oxidation of metallic cobalt in the powdered form.

1. B. Kievit and G. A. Lindsay, loc. cit.

Table II

The wave-lengths (X. U.), *the values of* $\frac{\nu}{R}$ *and* $\sqrt{\frac{\nu}{R}}$ *for the multiple structure of the*

		K	k_1	k_1'	k_2	k_2'	k_3	k_3'	k_4	k_4'	k_5
Cu(29)	λ	1377.6	1376.7	1374.3	1372.1	1369.5	1365.9	1362.4	1357.4	1353.2	1350.1
	$\Delta\lambda$	0	0.9	3.3	5.5	8.1	11.7	15.2	20.2	24.4	27.5
	$\frac{\nu}{R}$	661.47	661.93	663.08	664.14	665.39	667.14	668.83	671.32	673.41	674.97
	$\Delta\frac{\nu}{R}$	0	0.46	1.61	2.67	3.92	5.67	7.36	9.85	11.94	13.50
	ΔV	0	6.2	21.8	36.2	53.2	76.9	99.8	133.6	161.9	183.1
	$\sqrt{\frac{\nu}{R}}$	25.72	25.73	25.75	25.77	25.80	25.83	25.86	25.91	25.95	25.98
Ni(28)	λ	1484.8	1482.9	1480.8	1477.9	1475.3	1473.4	1472.4	1469.8	1464.7	1462.1
	$\Delta\lambda$	0	1.9	4.0	6.9	9.5	11.4	12.4	15.0	20.1	22.7
	$\frac{\nu}{R}$	613.73	614.53	615.39	616.59	617.69	618.50	618.92	619.99	622.17	623.24
	$\Delta\frac{\nu}{R}$	0	0.80	1.66	2.86	3.96	4.77	5.19	6.26	8.44	9.51
	ΔV	0	10.8	22.5	38.8	53.7	64.7	70.4	84.9	114.4	129.0
	$\sqrt{\frac{\nu}{R}}$	24.77	24.79	24.81	24.83	24.85	24.87	24.88	24.90	24.94	24.96
Co(27)	λ	1605.2	1603.2	1599.7	1596.5	1592.5	1590.2	1590.2	1587.1	1582.3	1577.5
	$\Delta\lambda$	0	2.0	5.5	8.7	12.7	15.0	15.0	18.1	22.9	27.7
	$\frac{\nu}{R}$	567.69	568.39	569.65	570.79	572.23	573.05	573.05	574.19	575.93	577.66
	$\Delta\frac{\nu}{R}$	0	0.70	1.96	3.10	4.54	5.36	5.36	6.50	8.24	9.97
	ΔV	0	9.5	26.6	42.0	61.6	72.7	72.7	88.1	111.7	135.2
	$\sqrt{\frac{\nu}{R}}$	23.83	23.84	23.87	23.89	23.92	23.94	23.94	23.96	24.00	24.04
Fe(26)	λ	1740.1	1738.1	1735.2	1733.3	1731.9	1729.9	1727.0	1722.5	1719.3	1715.7
	$\Delta\lambda$	0	2.0	4.9	6.8	8.2	10.2	13.1	17.6	20.8	24.4
	$\frac{\nu}{R}$	523.68	524.29	525.18	525.75	526.16	526.79	527.67	529.03	530.02	531.13
	$\Delta\frac{\nu}{R}$	0	0.61	1.50	2.07	2.48	3.11	3.99	5.35	6.34	7.45
	ΔV	0	8.3	20.3	28.1	33.6	42.2	54.1	72.5	86.0	101.0
	$\sqrt{\frac{\nu}{R}}$	22.88	22.90	22.92	22.93	22.94	22.95	22.97	23.00	23.02	23.05
Mn(25)	λ	1893.9	1890.3	1887.0	1883.0	1876.7	1872.5	1868.3	1864.2	1860.4	1856.1
	$\Delta\lambda$	0	3.6	6.9	10.9	17.2	21.4	25.6	29.7	33.5	37.8
	$\frac{\nu}{R}$	481.17	482.09	483.01	483.94	485.58	486.66	487.74	488.84	489.83	490.96
	$\Delta\frac{\nu}{R}$	0	0.92	1.84	2.77	4.41	5.49	6.57	7.67	8.66	9.79
	ΔV	0	12.5	25.0	37.6	59.8	74.4	89.1	104.0	117.4	132.8
	$\sqrt{\frac{\nu}{R}}$	21.94	21.96	21.98	22.00	22.04	22.06	22.09	22.11	22.13	22.16
Cr(24)	λ	2066.3	2062.4	2058.8	2056.4	2055.2	2051.9	2045.1	2040.1	2036.4	2031.7
	$\Delta\lambda$	0	3.9	7.5	9.9	11.1	14.4	21.2	26.2	29.9	34.6
	$\frac{\nu}{R}$	441.03	441.86	442.62	443.14	443.40	444.10	445.59	446.68	447.50	448.53
	$\Delta\frac{\nu}{R}$	0	0.83	1.59	2.11	2.37	3.07	4.56	5.65	6.47	7.50
	ΔV	0	11.3	21.6	28.6	32.1	41.6	61.8	76.6	87.7	101.7
	$\sqrt{\frac{\nu}{R}}$	21.00	21.02	21.04	21.05	21.06	21.07	21.11	21.14	21.16	21.18

K-absorption limits and their separation from the principal K-edge $\left\{\Delta\lambda,\ \Delta\frac{\nu}{R},\ \Delta V(\text{volts})\right\}$

k_5'	k_6	k_6'	k_7	k_7'	k_8	k_8'	k_9	k_9'	k_{10}	k_{10}'	k_{11}
1350.1	1346.1	1340.7	1333.7								
27.5	31.5	36.9	43.9								
674.97	676.95	679.71	683.25								
13.50	15.48	18.24	21.78								
183.1	209.9	247.3	295.3								
25.98	26.02	26.07	26.14								
1461.0	1458.0	1453.3	1450.0	1446.3	1442.7	1423.9	1415.3				
23.8	26.8	31.5	34.8	38.5	42.1	60.9	69.5				
623.73	625.02	627.05	628.48	630.05	631.66	639.96	643.86				
10.00	11.29	13.32	14.75	16.32	17.93	26.23	30.13				
135.6	153.1	180.6	200.0	221.3	243.1	355.7	408.6				
24.98	25.00	25.04	25.07	25.10	25.13	25.30	25.37				
1577.5	1572.3	1568.4	1564.7	1562.5	1556.9	1553.0	1545.9	1531.4	1522.1		
27.7	32.9	36.8	40.5	42.7	48.3	52.2	59.3	73.8	83.1		
577.66	579.57	581.01	582.41	583.20	585.30	586.77	589.49	595.07	598.69		
9.97	11.88	13.32	14.72	15.51	17.61	19.08	21.80	27.38	31.00		
135.2	161.1	180.6	199.6	210.3	238.8	258.7	295.6	371.3	420.4		
24.04	24.07	24.10	24.13	24.15	24.19	24.22	24.28	24.39	24.47		
1711.7	1708.4	1706.7	1702.0	1695.4	1682.5	1679.7	1664.2	1655.9	1640.7	1632.1	1618.5
28.4	31.7	33.4	38.1	44.7	57.6	60.4	76.0	84.2	99.4	108.0	121.6
532.39	533.42	533.93	535.40	537.51	541.61	542.53	547.60	550.32	555.42	558.36	563.05
8.71	9.74	10.25	11.72	13.83	17.93	18.85	23.92	26.64	31.74	34.68	39.37
118.1	132.1	139.0	158.9	187.5	243.1	255.6	324.4	361.2	430.4	470.3	533.9
23.07	23.10	23.11	23.14	23.18	23.27	23.29	23.40	23.46	23.57	23.63	23.73
1847.4	1841.3	1835.3	1829.6	1823.4	1817.8						
46.5	52.6	58.6	64.3	70.5	76.1						
493.28	494.91	496.53	498.08	499.76	501.30						
12.11	13.74	15.36	16.91	18.59	20.13						
164.2	186.3	208.3	229.3	252.1	273.0						
22.21	22.25	22.28	22.32	22.36	22.39						
2026.4	2020.8	2018.2	2009.9	2004.0	1984.8	1979.5	1958.4				
39.9	45.5	48.1	56.4	62.3	81.5	86.8	107.9				
449.70	450.94	451.53	453.38	454.73	459.12	460.36	465.32				
8.67	9.91	10.50	12.35	13.70	18.09	19.33	24.29				
117.6	134.4	142.4	167.5	185.8	245.3	262.1	329.4				
21.21	21.24	21.25	21.29	21.32	21.43	21.46	21.57				

III. Iron (26): With a tungsten anticathode, the strong WLl line appeared in the structure, so another plate was taken with molybdenum as the anticathode. But no new result could be obtained. New edges detected are denoted by (k_{10}) and (k_{11}).

IV. Manganese (25): A dozen plates were taken by various methods. A powder screen gave three or four secondary edges. Very thick screens gave no structure, and the main edge was very sharply limited and corresponded exactly to (K). The diffuse edge obtained with some other plates with no structure corresponded to (k_1). Some discrepancies were found between the multiple structure of pure manganese here obtained and that of Mn-Cu alloy reported by Kievit and Lindsay.

V. Chromium (24): Powder screens gave the same results as in the case of manganese in powder form. Metallic screens gave a new edge (k_2). Between (k_7') and (k_8) and also (k_8') and (k_9), there are faint discontinuities but these could not be precisely located.

Through this work, the gradual falling in intensity at the short wave-length side of the black structure line (namely at the secondary edge) is a very peculiar feature of the spectrograms and is shown also in the microphotometric curves especially in cobalt.

Part II. Theoretical Considerations

Several explanations to account for the origin of the extended multiple structure have been proposed by man investigators.

Here two reasonable hypotheses are taken into consideration.

The first hypothesis is that the multiple structure is the absorption discontinuities due to the absorption of a quantum of X-rays, resulting in the simultaneous ejection of many electrons from X-ray levels.

The second hypothesis is that the observed discontinuities are the K-ionization of an atom in which many electrons are lost owing to X-rays and photoelectrons from the same atom.

According to these hypotheses the following theoretical expectation for the wave-length or $\frac{\nu}{R}$-values of the multiple absorption edge can be made.

(I) The Energy Values by the First Hypothesis

If the validity of the $\{jj\}$ coupling can be accepted, the energy to remove two or more electrons simultaneously will be given approximately as follows:

Consider the change of state from a configuration.....$3s^2.\ 3p^6.\ 3d^{10}$ .....to the doubly ionized state.....$3s.\ 3p^5.\ 3d^{10}$.....for example. Various modes of changing the state can be imagined: (i) a $3s$ electron is removed, and then subsequently a $3p$ electron; (ii) a $3p$ electron is removed, and subsequently a $3s$ electron is removed; (iii) a $3s$ and a $3p$ electron are simultaneously removed. These modes of ionization are shown diagrammatically in the following figure. The long arrows indicate the processes of ionization through which one state may be reached from another by removal of electrons.

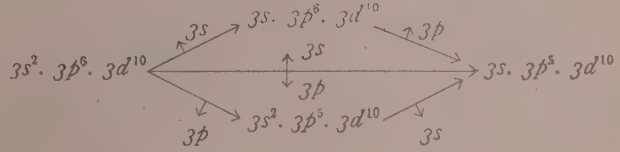

Merely the simultaneous ionization is in question here, but because of its complicated structure this can not be directly calculated. But if we assume that the energy difference is determined by the initial and final states only as in Born's cyclic process, the energy is equal in these three cases, and the required one is most easily calculated by taking case (i). Under such consideration, the energy required to remove a K and an M electron simultaneously from the same atom will be approximately equal to the energy required to remove the K electron plus the energy required to remove an M electron from the atom with atomic number one unit greater. Symbolically this is expressed as follows

$$K(Z)+M(Z)\equiv\underline{KM(Z)}<KM(Z)\lesssim K(Z)+M(Z+1)\equiv\overline{KM(Z)} \qquad (1)$$

where $KM(Z)$ means the energy required to remove a K and an M electron simultaneously from an atom with an atomic number Z, $K(Z)$ and $M(Z)$ the energies required to remove the K and M electrons respectively, and $\underline{KM(Z)}$ and $\overline{KM(Z)}$ signify the probable lower and upper limits of the energy in question.

Similarly the energy $M^2(Z)$ required to remove two M electrons from the atom will be given by

$$2M(Z)\equiv\underline{M^2(Z)}<M^2(Z)\lesssim M(Z)+M(Z+1)\equiv\overline{M^2(Z)}. \qquad (2)$$

Following Wentzel[1], let p_1, p_2, p_3.....be the number of electrons

1. G. Wentzel, Ann. d. Phys. **66**, 437 (1921)

in the K, L, M.....shell of the normal atom, then the energy of the atom will be given as a function of p_1, p_2, p_3.....

Then we have

$$K(Z)=W(p_1-1, p_2.....)-W(p_1, p_2, p_3.....)$$
$$=-\frac{\partial W}{\partial p_1}+\frac{1}{2!}\frac{\partial^2 W}{\partial p_1^2}-\frac{1}{3!}\frac{\partial^3 W}{\partial p_1^3}+..... \quad (3)$$

and

$$M(Z)=W(p_1, p_2, p_3-1.....)-W(p_1, p_2, p_3.....)$$
$$=-\frac{\partial W}{\partial p_3}-\frac{1}{2!}\frac{\partial^2 W}{\partial p_3^2}-\frac{1}{3!}\frac{\partial^3 W}{\partial p_3^3}+..... \quad (4)$$

In general, let the notation $K^{d_1}L^{d_2}M^{d_3}$ be the term values equivalent to the energy of an atom which has had d_1 electrons removed from the K shell, d_2 electrons removed from the L shell, and d_3 electrons from the M shell and so on, then

$$K^{d_1}L^{d_2}M^{d_3}.....=W(p_1-d_1, p_2-d_2, p_3-d_3,...)-W(p_1, p_2, p_3...)$$
$$=-\sum_i d_i\frac{\partial W}{\partial p_i}+\frac{1}{2!}\sum_{ik} d_i d_k\frac{\partial^2 W}{\partial p_i\partial p_k}$$
$$-\frac{1}{3!}\sum_{ikl} d_i d_k d_l\frac{\partial^3 W}{\partial p_i\partial p_k\partial p_l}+..... \quad (5)$$

Using this result I derived the simple expression,

$$K'M^n(Z)=K(Z)-n\left(M(Z)+\frac{\partial^2 W}{\partial p_1\partial p_3}\right)-\frac{n(n-1)}{2}\frac{\partial^2 W}{\partial p_3^2}. \quad (6)$$

Although the values of $\frac{\partial^2 W}{\partial p_1\partial p_3}$, $\frac{\partial^2 W}{\partial p_3^2}$ are unknown, this equation serves to clear the matter to some extent.

The vertical lines in Fig. 5 give the separation for the elements from Cu(29) to Cr(24) in $\frac{\nu}{R}$-units between the principal edge and the various secondary edges calculated according to the above principle.

The value of the M levels in Fig. 5 are taken from the paper by E. C. Stoner[1], who has calculated the term values using Thoraeus'[2] data. The values for Ga(30) are calculated by interpolation from Moseley's diagram.

---

1. E. C. Stoner, Phil. Mag. **2**. 97 (1926)
2. Thoraeus, Phil. Mag. **1**. 312 (1926)

Fig. 5

Calculated energy level diagram for multiple X-ray ionization.

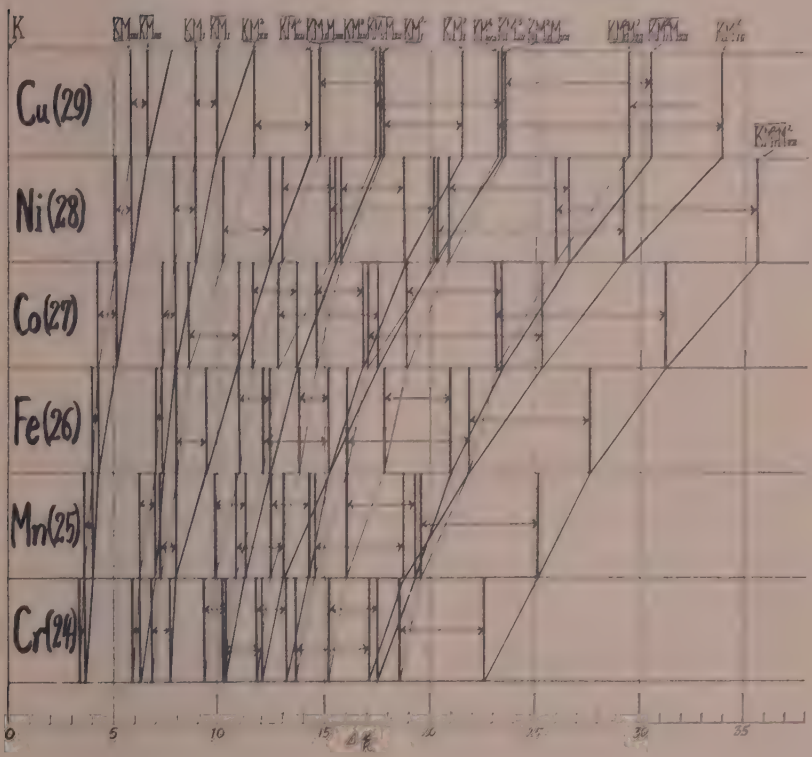

(II) The Energy Values by the Second Hypothesis

This hypothesis regards the observed structure as due to the ejection of a K electron from the multiply ionized atom in various shells.

Let $Kl(Z)$ be the energy required to eject a K electron from the singly ionized atom in the L shell, then we have as a first approximation.

$$Kl(Z) < \overline{Kl(Z)} = K(Z) + L(Z+1) - L(Z). \qquad (7)$$

Similarly let $Kl^2(Z)$ be the K ionization potential for the doubly ionized atom in the L shell,

$$Kl^2(Z) < \overline{Kl^2(Z)} = K(Z) + L(Z+2) - L(Z). \qquad (8)$$

Following Wentzel[1], I have

$$Kl^m(Z) \equiv KL^m - L^m = K + m\frac{\partial^2 W}{\partial p_1 \partial p_2} .$$

Let the total energy of the normal atom be equal to

$$W = -\sum_k p_k \frac{\left(Z - \sum_{i=1}^{k-1} p_i - s_k\right)^2}{k^2}, \qquad (9)$$

where s_k is a screening constant, and we obtain the formula:

$$\frac{\partial^2 W}{\partial p_1 \partial p_n} = \frac{2}{n}\left\{\frac{\left(Z - \sum_{i=1}^{n-1} p_i - s_n\right)}{n} - \frac{p_n}{n}\frac{\partial s_n}{\partial p_n} - n\sum_{k=n+1}\frac{p_k}{k^2}\right\}. \qquad (10)$$

For example,

$$\frac{\partial^2 W}{\partial p_1 \partial p_2} = \left\{\frac{Z - p_1' - s_2}{2} - \frac{p_2}{2}\frac{\partial s_2}{\partial p_2} - \frac{2p_3}{3^2} - \frac{2p_4}{4^2}\right\}, \qquad (11)$$

for the atom of the iron group ionized in the shell $2p$. Here p_1' contains the p of $1s$ and $2s$.

The first term of the right hand side of the equation is obtained from the value of $\sqrt{\frac{\nu}{R}}$ of $L_{II}(Z)$ of the atom in question as a first approximation[2].

The value of $\frac{\partial s_2}{\partial p_2}$ is 0.5 also as a first approximation. This is correct for a spherical shell at least.

The values of $\frac{\partial^2 W}{\partial p_1 \partial p_2}$ computed from this equation are respectively

2.06, 2 30, 2.45, 2.60, 2.74, and 2.77 in $\frac{\nu}{R}$-units for Cr, Mn, Fe, Co, Ni, and Cu respectively.

And these figures give the values of separation from the principal K-edge.

The values (designated by $\underline{Kl}-K$) and the values of $\overline{\underline{Kl}}-K$ and $\overline{\underline{Kl}^2}-K$ computed from equations (7) and (8) respectively, are plotted in Fig. 6.

The term KL ($1s.\ 2s^2.\ 2p^5$) will be ^1P and ^3P.

Real value will exist between $\underline{Kl}$-K and $\overline{\underline{Kl}}$-$K$, or very close to them.

---

1. G. Wentzel, l. c.
2. This point will be discussed elsewhere.

Fig. 6

The theoretical value of separation. The K edge of an atom that has lost one or more $2p$ electrons—The principal edge.

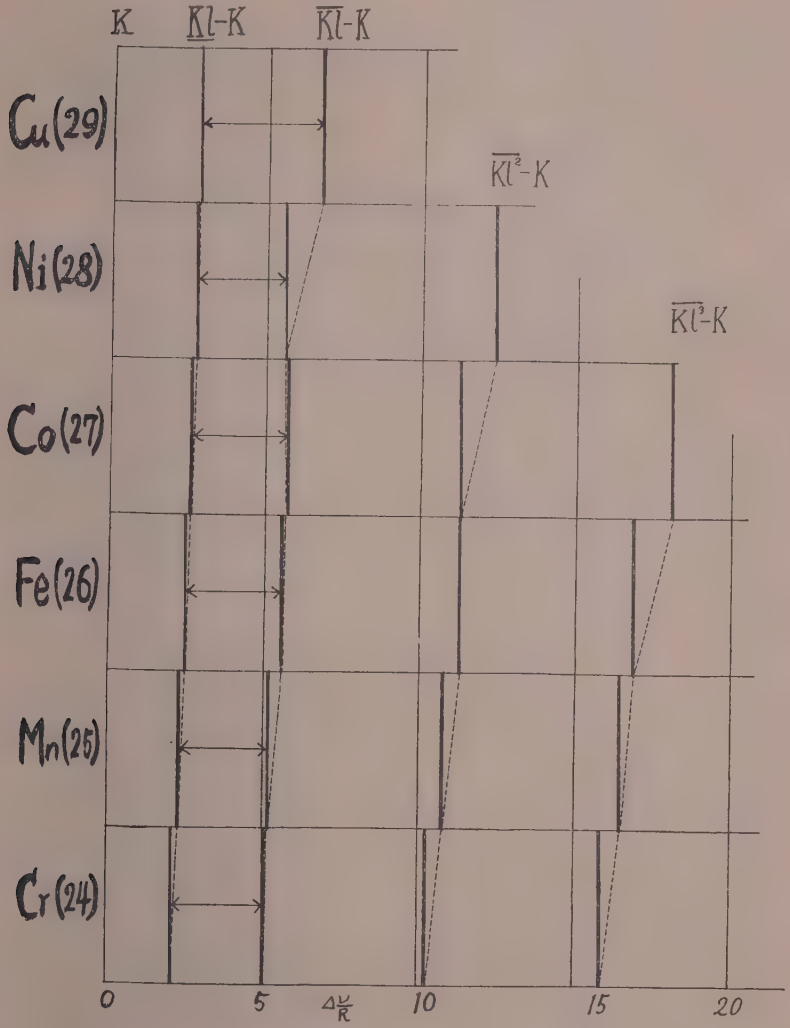

(III) Remarks

By the preceding line of argument, only approximate values can be secured for the energy levels. Hence the more detailed points which must be taken into consideration will be mentioned here.

(1) *Change of term values with the coupling between electrons*

It has been assumed that the $\{jj\}$ coupling may hold true, but this is not always the case.

For electrons of the same group in light elements, the $\{LS\}$ coupling may occur. Under these circumstances, if a K-electron and two $M_{II,III}(3p)$ electrons are ejected from an atom, there will be present various levels deviating from the value $KM^2_{II,III}(Z)$, because even if the coupling between K and M electrons may be $\{jj\}$, that between two $3p$ electrons may be recognized as approaching the $\{LS\}$ coupling, which will give rise to fairly widely separated energy levels such as $^1S_0$, $^1D_2$, and $^3P_{0,1,2}$. Recently S. Goudsmit[1] derived the expressions giving the change in the positions of the energy levels with change in electron coupling for the configuration p^4. Applying his theory in the case of X-rays, I attempted some estimations. As an example, for nickel, the triplet separation must be equal to 0.10 in $\frac{\nu}{R}$-units. Let the separation between $^1S_0$ and $^3P_{0,1,2}$ or $^1D_2$ and $^3P_{0,1,2}$ become ten times this triplet separation, then the total separation will become 1.6. But the coupling strength cannot be accurately obtained and this is only a rough estimation. But these values will deviate fairly far from that of a single $KM^2_{II,III}$ term. Hence there is a possibility that *many* absorption edges will be *experimentally* secured from one configuration of electrons.

(2) *The end orbits of electrons in the process of absorption*

In contrast to Kievit and Lindsay, in the foregoing discussion I have assumed that the electrons are completely taken from the atom, taking into consideration the fact that the ionization potential of the metallic element is small. Actually in the case of a metal in the solid state, there are free electrons present, and we cannot predict how many and which electrons are free. Accordingly we cannot precisely decide whether a metal consists of atoms or ions. Hence the determination of the end orbit is especially difficult. But this can be done in the case of gaseous atoms, using optical deta. One word more may be said in connection to this point. It is known that for every valency electron i (i=1, 2, 3.....) that takes part in the change of state of the atom the selection rule for l is $\sum_i \Delta l_i = \pm 1$, and not $\Delta l_i = \pm 1$. In the case of X-ray spectroscopy, if we can obtain the multiple structure of the absorption spectra in gaseous atoms, and can

1. S. Goudsmit, Phys. Rev. **35**, 1325 (1930)

accurately determine it, it will be interesting to test whether the above selection rule holds or not also in the process of absorption in the X-ray region.

(3) In constructing Fig. 6 only *3s* and *3p* electrons were taken into consideration and *3d* or *4s* electrons were neglected. This must cause slight discrepancies between the calculated and the observed values.

Conclusion

In spite of the presence of the above-cited difficulties, there are some facts explained qualitatively at least. Comparison of Fig. 4 and Fig. 5 shows that coincidence of the value is frequently found. The intersections of the curves $\overline{KM_1^2}$ and $\overline{KM_{II,III}^2}$, $\overline{KM_1^2M_{II,III}}$ and $\overline{KM_{II,III}^2}$ are interesting, and the irregularities that are found in the case of Fe and Mn in Fig. 4 can be predicted.

The fact that a gradual decrease in intensity towards the short wave-length side is often observed in many spectrograms, can be interpreted by the idea of multiplets in the case of $\{LS\}$ coupling.

In comparing Fig. 4 and Fig. 6, one of the edges (k_2), (k_3) (k_4), and (k_5) is to be regarded as due to a singly ionized atom in L shell. The facts that the related black lines of similar intensity and structure nearly fall into the same vertical lines in Fig. 4 (that is variations with the atomic number are small), and that there is a gradual fall in intensity at the short wave-length side, are due to the term multiplicities of ^1S and ^3S for the configuration $1s\ 2s\ 2p^6$ and ^1P, ^3P for $1s\ 2s^2\ 2p^5$ and so on. The precise theoretical determination of the energies required for multiple ionization of the atom is difficult, but the probable explanation seems to be provided by these two hypotheses to some extent. So on the whole, it is to be supposed that in the process of absorption of X-rays these two different types of absorption really occur, and that the spectrograms are the result of superposition of such a complex process.

But here arises two questions of probability:

(1) The probability of multiple electron jumps owing to the absorption of a single quantum.

(2) The probability of the atom being brought into the state of multiple ionization by X-rays and photoelectrons from the same atom, and especially the length of stay (Verweilzeit).

The problem should be solved by the new quantum mechanics, and this is intimately related to the explanation of the spark lines in the X-ray emission spectra.

In conclusion, the writer wishes to express his sincere thanks to Prof. M. Ishino for his kind guidance and for the interest he has taken in this research.

Plate Figure

Fig. 2. Multiple structure in the K absorption spectra of metallic elements (A)—(H)

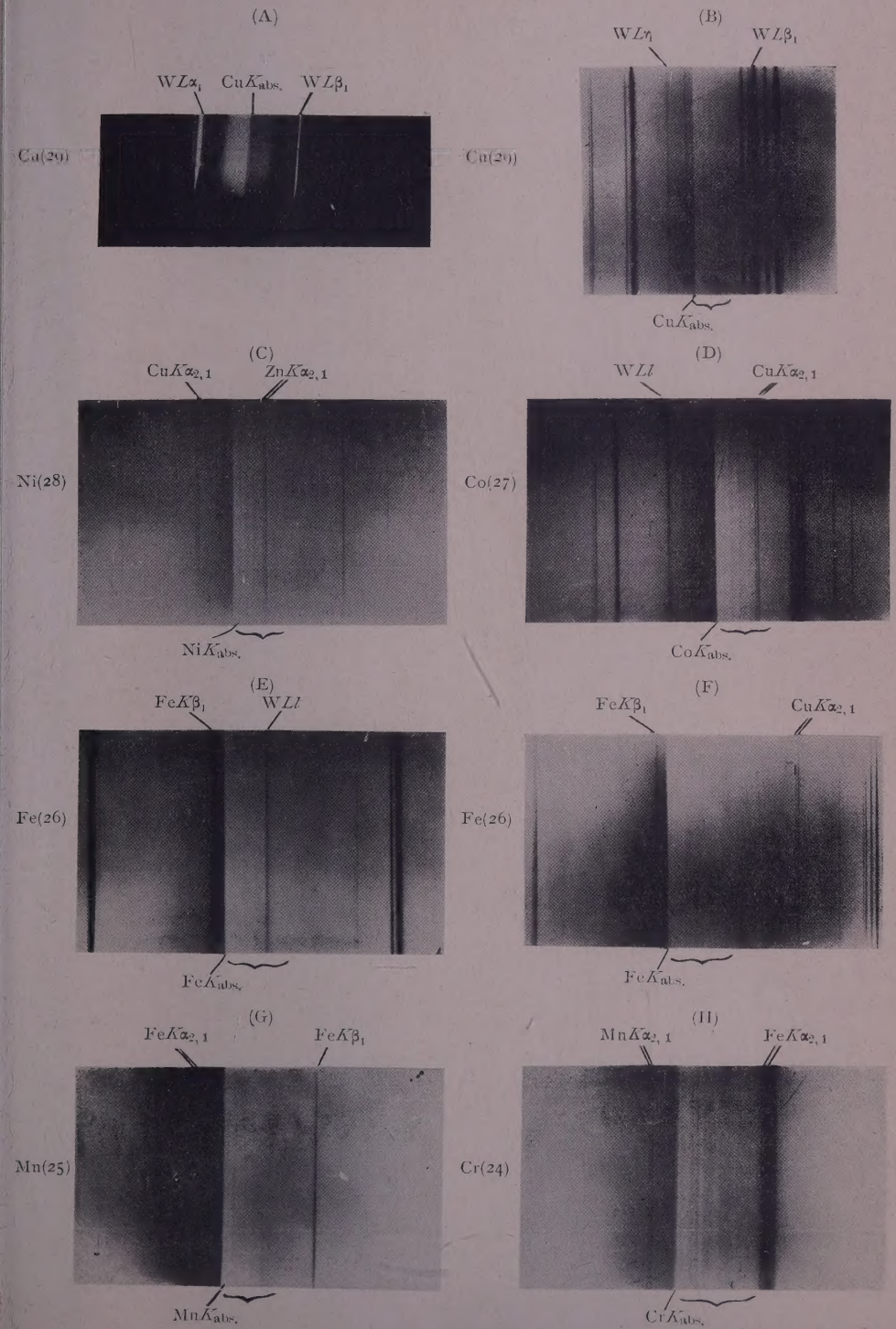

Vol. XIV, No. 5, Published September 30, 1931

Price - - - - Yen 1.30

These Memoirs are on Sale at

MARUZEN COMPANY, LTD.

TOKYO, OSAKA, KYOTO, NAGOYA, YOKOHAMA,
FUKUOKA & SENDAI

昭和六年九月二十五日印刷
昭和六年九月三十日發行

編纂兼發行者　京都帝國大學理學部

印刷者　須磨勘兵衞
京都市下京區北小路通新町西

印刷所　內外出版印刷株式會社
京都市下京區西洞院七條南

賣捌所　丸善株式會社
東京、大阪、京都、名古屋、横濱、福岡、仙臺

CONTENTS

On a Unified Theory of Gravitational and Electromagnetic Fields

By Shūjiro Kunii 195

Experimental Studies on the Sound of a Japanese Hanging Fire-Bell

By Ichiro Aoki 213

Some Strange Oscillatory Discharge-Figures on Photographic Plates

By Tatsumi Terada 219

X-Ray Diagram Lines Strongly Absorbed in the Absorption Spectra

By Suekichi Kawata 227

On the Multiple Structure in the K X-ray Absorption Spectra of the Metallic Elements Cr, Mn, Fe, Co, Ni and Cu

By Masao Sawada 229